Atlantic Major Hurricanes, 1995–2005—Characteristics Based on Best-Track, Aircraft, and IR Images

RAYMOND M. ZEHR AND JOHN A. KNAFF

NOAA/NESDIS, Fort Collins, Colorado

(Manuscript received 28 August 2006, in final form 1 May 2007)

ABSTRACT

The Atlantic major hurricanes during the period of 1995–2005 are examined using best-track data, aircraft-based observations of central pressure, and infrared (IR) satellite images. There were 45 Atlantic major hurricanes (Saffir–Simpson category 3 or higher) during this 11-yr period, which is well above the long-term average. Descriptive statistics (e.g., average, variability, and range) of various characteristics are presented, including intensity, intensification rate, major hurricane duration, location, storm motion, size, and landfall observations. IR images are shown along with IR-derived quantities such as the digital Dvorak technique intensity and IR-defined cold cloud areas. In addition to the satellite intensity estimates, the associated component IR temperatures are documented. A pressure–wind relationship is evaluated, and the deviations of maximum intensity measurements from the pressure–wind relationship are discussed.

The Atlantic major hurricane activity of the 1995–2005 period distinctly exceeds the long-term average; however, the average location where major hurricanes reach maximum intensity has not changed. The maximum intensity for each 1995–2005 Atlantic major hurricane is given both as the highest maximum surface wind (Vmax) and the lowest minimum sea level pressure (MSLP). Comparisons are made to other Atlantic major hurricanes with low MSLP back to 1950. Maximum 24-h intensification rates average 21.1 m s^{-1} day^{-1} and range up to 48.8 m s^{-1} day^{-1} in terms of Vmax. The largest 24-h MSLP decreases average 34.2 hPa and range from 15 to 97 hPa. Major hurricane duration averages 2.7 days with a maximum of 10 days. Hurricane size, as given by the average radius of gale force wind at maximum intensity, averages 250.8 km and has an extremely large range from 92.5 to 427.4 km.

1. Introduction

During the 11-yr period of 1995–2005, there were 45 major hurricanes in the Atlantic basin. Major hurricanes are those that attain Saffir–Simpson category 3 or higher (Simpson 1974). Category 3 is defined by maximum surface wind speed equal to or greater than 51.4 m s^{-1} (100 kt). The Atlantic basin includes the North Atlantic Ocean, Caribbean Sea, and Gulf of Mexico. A distinct upturn in the frequency of Atlantic major hurricanes has occurred since 1995, with an annual average of 4.1 major hurricanes (1995–2005), compared with the 1950–2005 average of 2.7. Longer-term climatology gives an annual average of 1.9 Atlantic major hurricanes (Elsner and Kara 1999). This resurgence of Atlantic major hurricanes was noted by Wilson (1999) and discussed in subsequent papers by Elsner et al. (2000a) and Goldenberg et al. (2001). The North Atlantic Oscillation (NAO) has been shown to be an influence on Atlantic major hurricane activity (Elsner et al. 2000b). Gray et al. (2005) attribute this upswing in activity to multidecadal fluctuations in the Atlantic Ocean thermohaline circulation.

Previous studies have explored trends in tropical cyclone records and associated El Niño–Southern Oscillation (ENSO) and quasi-biennial oscillation (QBO) indicators with regard to the global distribution and frequency of tropical cyclones (Gray 1984; Goldenberg and Shapiro 1996; Landsea et al. 1996; Elsner et al. 1999; Elsner and Kara 1999; Saunders et al. 2000; Elsner et al. 2004). Emanuel (2005) and Webster et al. (2005) discuss evidence for warming sea surface temperatures associated with anthropogenic climate change, and resulting increases in tropical cyclone intensity and frequency. Our paper does not address these important issues but instead is focused on presenting a descriptive observational overview of Atlantic major hurricane characteristics.

Corresponding author address: Ray Zehr, CIRA/Colorado State University, W. LaPorte Ave., Fort Collins, CO 80523.
E-mail: Ray.Zehr@noaa.gov

DOI: 10.1175/2007JCLI1652.1

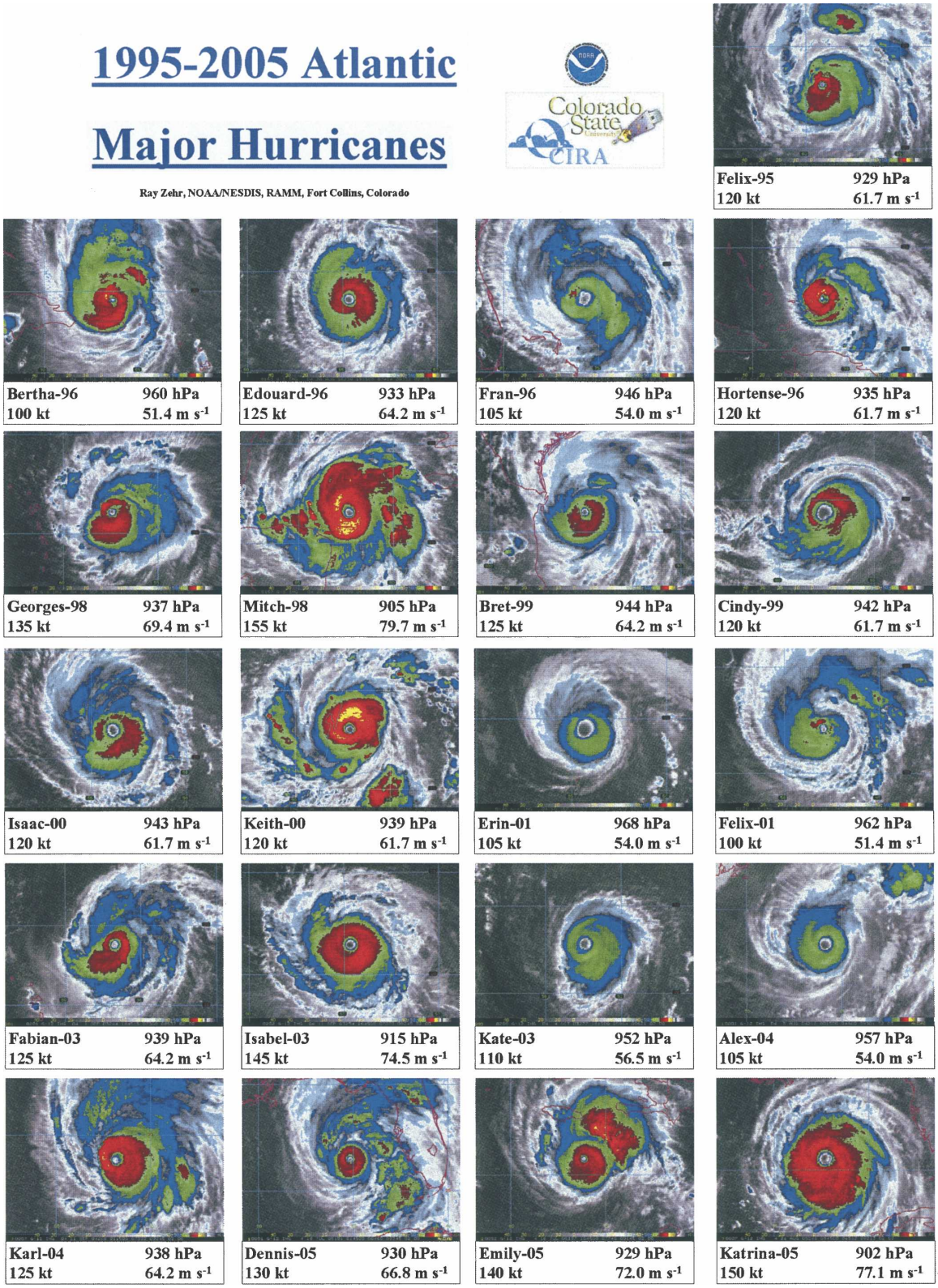

FIG. 1. Color enhanced IR images of each 1995–2005 Atlantic major hurricane, near the time of maximum intensity. The blue shades indicate IR temperatures −50° to −59°C, green −60° to −69°C, red −70° to −79°C, and yellow −80°C and colder. Each image is a hurricane-centered 4-km resolution Mercator remapped 1280 km × 960 km image. They are ordered according to date.

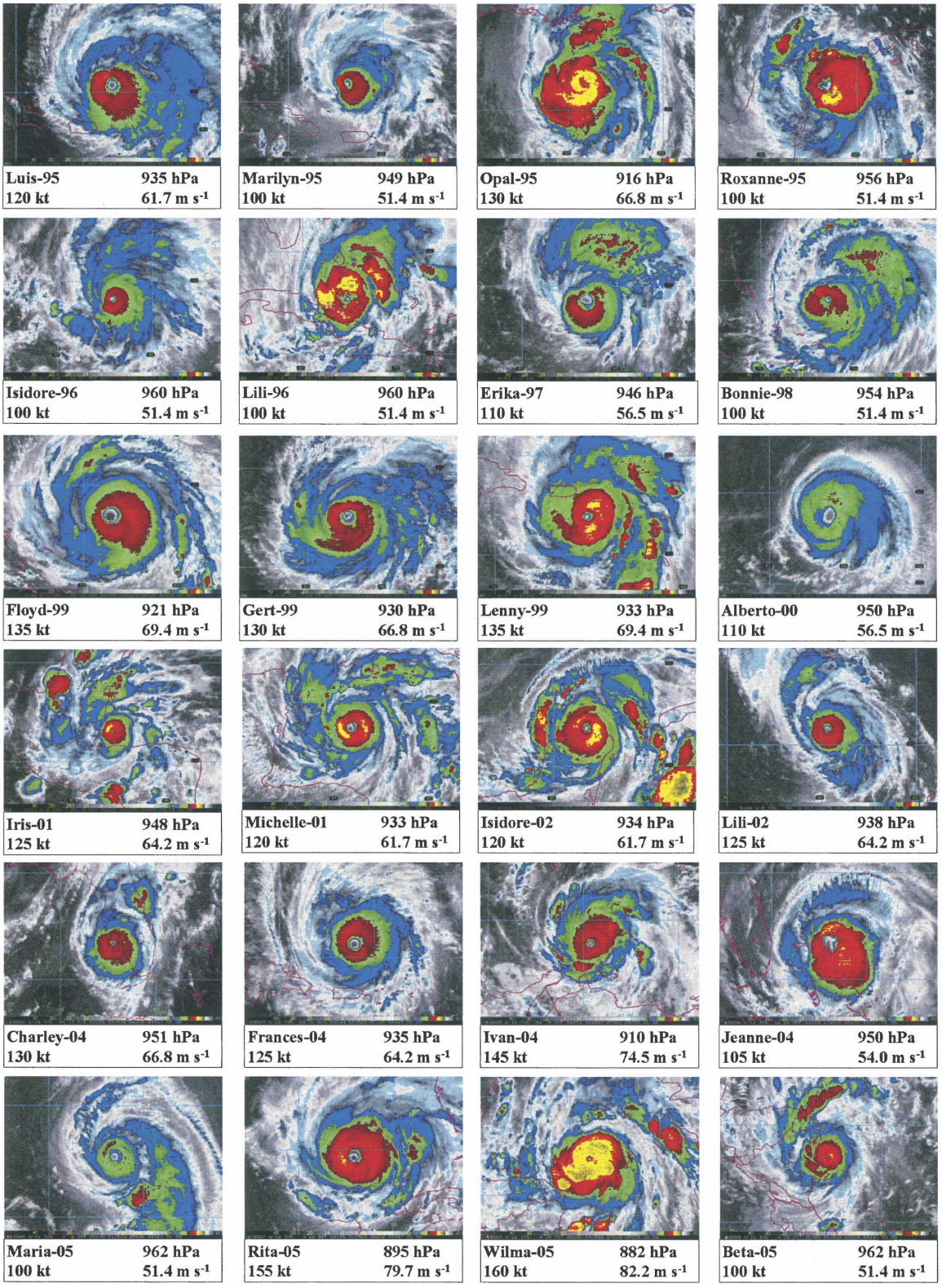

FIG. 1. (*Continued*)

The 11-yr 1995–2005 sample is used to document basic characteristics of Atlantic major hurricanes. The 1995–2005 period was chosen because of the increased frequency of major hurricanes and the availability of the IR satellite archive (Zehr 2000; Mueller et al. 2006). Using "best track" data (Jarvinen and Neumann 1979), ordered lists of various parameters associated with each of the 45 major hurricanes have been compiled. For example, the lowest minimum sea level pressure (MSLP) with each hurricane ranges from 882 hPa with Wilma (2005) to 968 hPa with Hurricane Erin (2001). Along with the best-track data, minimum sea level pressure estimates from reconnaissance aircraft, operational wind radii estimates, and landfall data from the Tropical Prediction Center are used to quantitatively describe the characteristics of the major Atlantic hurricanes during this period. The geostationary satellite infrared (IR) temperature data provide images and satellite-derived intensity estimates (Dvorak 1984; Velden et al. 1998).

Figure 1 shows color-enhanced IR images of each of the 45 Atlantic major hurricanes from 1995 to 2005. They are shown from left to right from the top, in order of occurrence as hurricane-centered, 4-km-resolution remapped Mercator images near the time of maximum intensity. The common format allows a quick evaluation of both common features and large differences. For example, Hurricane Iris (2001) has a much smaller cloud pattern compared with Hurricane Floyd (1999). All of them have well-defined eyes. They all have associated deep clouds with IR temperatures colder than –60°C. Ninety-three percent have some cloud area colder than –70°C, and 44% have pixels colder than –80°C.

2. By year

Figure 2 shows the number of Atlantic major hurricanes by year, beginning with 1950. The period 1995–2005 is comparable to the 1950s and early 1960s in number of major hurricanes, while the years between had fewer major hurricanes. For the 1995–2005 period (Fig. 2b), the 2004–05 seasons combined for 13 major hurricanes, while 1997 and 2002 were the only years below the 1950–2005 average of 2.7. The years 1997 and 2002 were El Niño years, usually associated with below-average Atlantic hurricane activity (Gray 1984; Landsea et al. 1999).

3. Within season distribution

The frequency distribution of the 1995–2005 Atlantic major hurricane best-track time periods according to

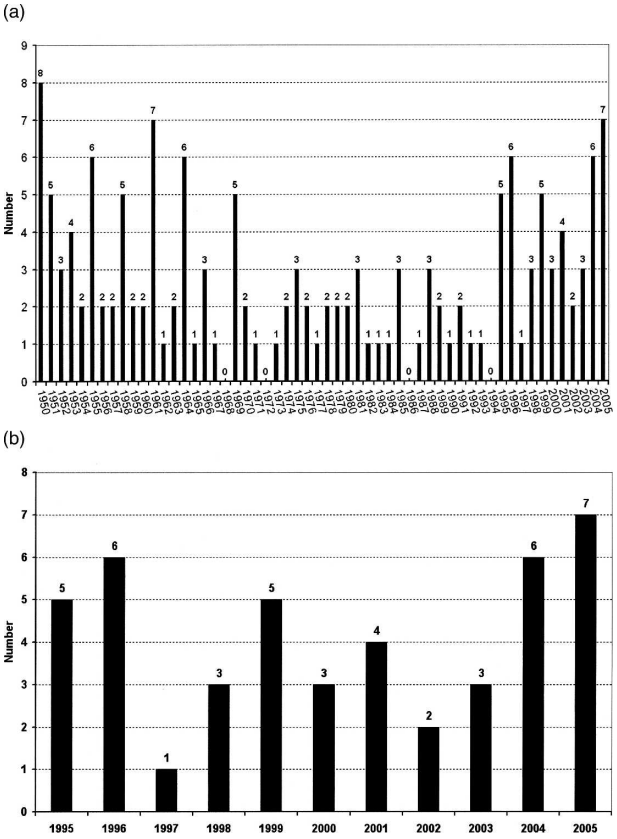

FIG. 2. Number of Atlantic major hurricanes by year: (a) 1950–2005 and (b) 1995–2005.

Julian day shows that 72% occurred between Julian day 235 (23 August 23; 22 August in leap year) and Julian day 268 (25 September; 24 September in leap year). This intraseasonal distribution agrees closely with the Atlantic major hurricane climatology given by Landsea (1993) and Elsner and Kara (1999). The overall average Atlantic tropical cyclone occurrence shows a distinct increase in early August, a mid-September peak and nearly all activity occurring in June through November (Neumann et al. 1999). The intraseasonal distribution of major hurricanes is more concentrated, during the more active portion of the season in late August to late September. The 1995–2005 Atlantic major hurricanes also have this characteristic active period. Early and late season major hurricanes were observed in 1995–2005, with the earliest being Hurricane Dennis on 7 July 2005, and the latest being Hurricane Lenny on 18 November 1999.

4. Location

The map in Fig. 3 shows where each hurricane was located at the time of its maximum intensity. Four of the category 5 hurricanes were located rather close to-

FIG. 3. Location of the 1995–2005 Atlantic major hurricanes at the time of their maximum intensity, according to lowest MSLP from the best-track data. Category 5 hurricanes are plotted in red, category 4 in blue, and category 3 in green. The average location is denoted by the red ×.

gether in the Caribbean, and two were in the Gulf of Mexico. However, category 5 Hurricane Isabel (2003) was located in the mid-Atlantic. Hurricane Bret (1999) was farthest west, Hurricane Alex (2004) farthest north, Hurricane Beta (2005) farthest south, and Hurricane Isidore (1996) at the easternmost location. The average latitude–longitude of the 45 major hurricanes at maximum intensity is 23.5°N, 70.7°W, about 700 km northwest of Puerto Rico, and 1000 km east-southeast of Miami, Florida. This position is very close to the 1950–2005 mean position of major hurricane maximum intensity of 24.3°N, 71.3°W. The distribution of 1995–2005 major hurricanes in Fig. 3 is consistent with the general location of Atlantic tropical cyclones (Neumann et al. 1999) except that at maximum intensity, the locations are all south of 40°N. A more complete view of Atlantic major hurricane climatology by location according to origin and dissipation points, along with tracks, can be found in Elsner and Kara (1999).

5. Intensity

a. Maximum surface wind speed

Hurricane intensity is expressed as the associated maximum surface wind speed (Vmax) or as the minimum sea level pressure. The highest Vmax values for each case are plotted in Fig. 4, in knots (kt) with a scale in standard units of meters per second. It should be noted that best-track files give maximum surface wind speed in 5-kt increments, and for this reason the unit of knots will be used when discussing intensity for the remainder of the paper. Using the best-track data, major hurricanes are those with Vmax equal to or greater than 100 kt (51.4 m s^{-1}). The best-track measurements are at 6-h intervals, which may not always capture the maximum intensity. However, Tropical Prediction Center archives also include an estimate of maximum intensity (highest Vmax) and its time of occurrence.

Applying Saffir–Simpson intensity categories to the

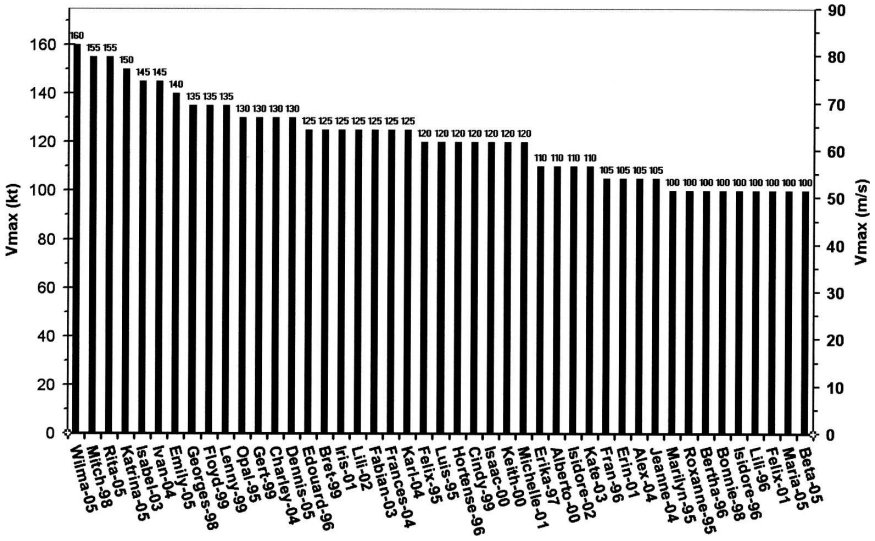

FIG. 4. Highest maximum surface wind speed (Vmax) for each 1995–2005 Atlantic major hurricane, from the best-track data. A scale for m s^{-1} is shown on the right. The average highest Vmax is 121.1 kt (62.2 m s^{-1}) with a standard deviation of 17.0 kt (8.7 m s^{-1}).

1995–2005 Atlantic hurricanes, there are seven (16%) category 5 hurricanes, 21 (47%) category 4, and 17 (38%) category 3 hurricanes. The long-term (1950–2005) average distribution of highest Vmax is as follows: category 5, 16%; category 4, 37%; and category 3, 47%.

Wilma (2005) was the most intense major hurricane with Vmax of 160 kt (82.2 ms^{-1}), while Hurricanes Mitch (1998) and Rita (2005) had Vmax of 155 kt (79.7 m s^{-1}). The 1995–2005 major hurricane peak Vmax average is 121.1 kt (62.2 m s^{-1}), compared with the long-term (1950–2005) average of 118.6 kt (60.9 m s^{-1}).

b. Minimum sea level pressure

The lowest MSLPs for each 1995–2005 Atlantic major hurricane are plotted in Fig. 5, and the 10 lowest are listed in Table 1. The MSLP in increments of 1 hPa more effectively differentiates intensities among the cases than the Vmax. The 10 lowest MSLP's for 1995–2005 are all less than 930 hPa. For comparison, and to put the more recent hurricanes in a historical perspective, Table 2 lists all of the 1950–2005 Atlantic hurricanes with MSLPs that went below 930 hPa. Hurricane

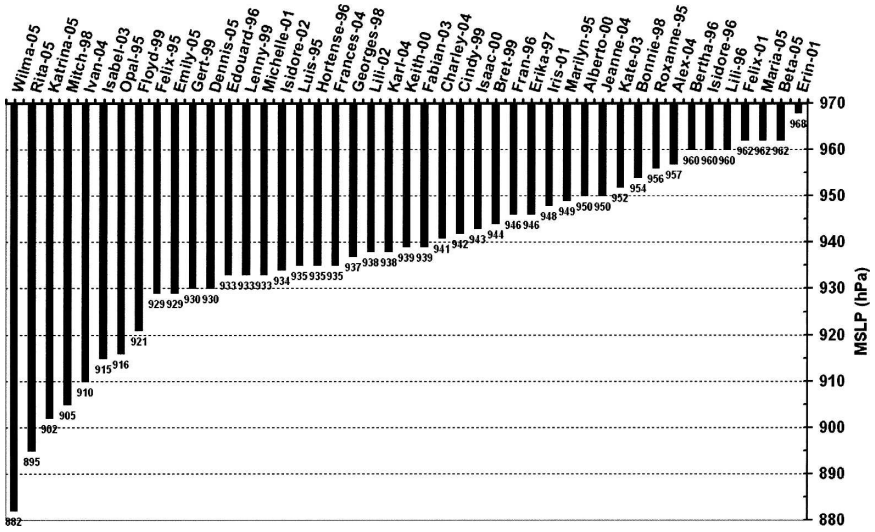

FIG. 5. Lowest MSLP for each 1995–2005 Atlantic major hurricane, from the best-track data. The average is 937.9 hPa with a standard deviation of 18.9.

TABLE 1. Ten lowest MSLPs (hPa) with 1995–2005 Atlantic major hurricanes.

Hurricane	MSLP
1) Wilma (2005)	882
2) Rita (2005)	895
3) Katrina (2005)	902
4) Mitch (1998)	905
5) Ivan (2004)	910
6) Isabel (2003)	915
7) Opal (1995)	916
8) Floyd (1999)	921
9) Felix (1995)	929
10) Emily (2005)	929

Wilma (2005) had the lowest MSLP of 882 hPa, which broke the previous all-time record for Atlantic hurricanes of 888 hPa with Hurricane Gilbert in 1988 (Willoughby et al. 1989). Elsner and Kara (1999) provide documentation on sea level pressure observed with U.S. landfalling major hurricanes prior to 1950.

c. Pressure–wind relationship

It is important to make note of the source of the best-track MSLP as to whether it was based on an aircraft measurement or a satellite intensity estimate. With the satellite estimate, a standard pressure–wind relationship (Dvorak 1984) is used to assign the MSLP. The "pressure–wind relationship" quantitatively associates Vmax and MSLP. With the sample of 45 lowest MSLP, 32 cases were based on aircraft measurements, while 13 were from satellite intensity estimates.

Figure 6 shows the lowest MSLP versus highest Vmax for each of the 45 cases, along with a line depicting the Dvorak pressure–wind relationship. The points that are aligned near this line include those 13 cases for which aircraft observations were not available at the time maximum intensity. The scatter of the independently estimated MSLP shows the impact of aircraft data. As additional illustration of the impact of the aircraft data, the same thing is plotted in Fig. 7 for the 1995–2005 eastern Pacific major hurricanes, which are not routinely observed with aircraft. The single outlier in Fig. 7 was in fact supported by aircraft data with Hurricane Juliette in 2001. An aircraft mission was flown near the time of maximum intensity.

d. Delta-p

The data in Figs. 4–6 show that deviations from the pressure–wind relationship not only influence a hurricane's intensity ranking, but also define a measurable hurricane characteristic according to those deviations. For example, Hurricane Georges (1998) is in the top 10 in terms of its Vmax of 135 kt (69.4 m s^{-1}), while ranking 20th in terms of MSLP (937 hPa). In contrast, Hurricane Felix (1995) is in the 10 most intense hurricanes with an MSLP of 929 hPa, while its Vmax is at the median value of 120 kt (61.7 m s^{-1}).

Figure 8 is a plot of the deviations of observed MSLP from the MSLP specified by the Dvorak (1984) pressure–wind relationship and the Vmax, using the data from Fig. 6. Hurricane Wilma (2005) with an MSLP of 882 hPa, has a Vmax of 160 kt (82.2 m s^{-1}) that the pressure–wind relationship associates with 900.8 hPa, giving the –18.8 hPa deviation shown in Fig. 8. Similarly, Hurricanes Opal (1995), Felix (1995), and Isidore (2002) have comparable deviations of the same sign and magnitude. In contrast, Hurricane Erin (2001) has an MSLP of 968 hPa, and the MSLP computed by applying the pressure–wind relationship to a Vmax of 105 kt (54.0 m s^{-1}) is 956 hPa, giving a +12 hPa deviation. Hurricanes Georges (1998), Charley (2004), and Iris (2001) have similar deviations in the +8 to +10 hPa range.

Comparing the two major hurricanes in 2002, Lili is the more intense hurricane in terms of Vmax with 125 kt (64.2 m s^{-1}) versus Isidore's 110 kt (56.5 m s^{-1}). However, if MSLP is used to measure intensity, Isidore is the more intense hurricane with 934 hPa compared to Lili's 938 hPa.

TABLE 2. Lowest MSLPs (hPa) with 1950–2005 Atlantic hurricanes, with MSLP less than 930 hPa.

Hurricane	MSLP
1) Wilma (2005)	882
2) Gilbert (1988)	888
3) Rita (2005)	895
4) Allen (1980)	899
5) Katrina (2005)	902
6) Camille (1969)	905
7) Mitch (1998)	905
8) Ivan (2004)	910
9) Janet (1955)	914
10) Isabel (2003)	915
11) Opal (1995)	916
12) Hugo (1989)	918
13) Hattie (1961)	920
14) Gloria (1985	920
15) Floyd (1999)	921
16) Andrew (1992)	922
17) Beulah (1967)	923
18) David (1979)	924
19) Anita (1977)	926
20) Esther (1961)	927
21) Gabrielle (1989)	927
22) Carmen (1974)	928
23) Carol (1953)	929
24) Inez (1966)	929
25) Felix (1995)	929
26) Emily (2005)	929

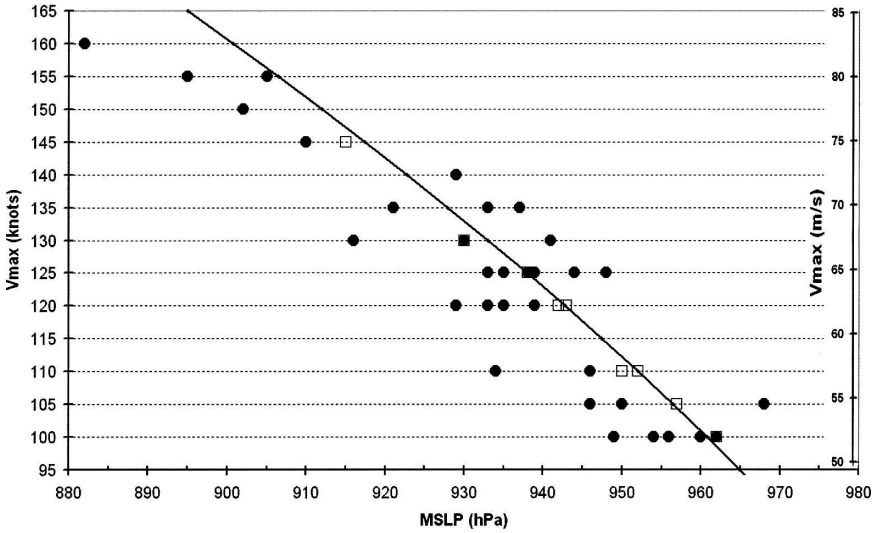

FIG. 6. Scatterplot of highest Vmax and lowest MSLP for each 1995–2005 Atlantic major hurricane from the best-track data. The line is the pressure–wind relationship from Dvorak (1984). Those cases that were measured by aircraft are plotted as circles, and those with no aircraft observations are squares. Some of the points are for multiple cases with identical values.

The best-track datasets provide a measure of how closely a hurricane's Vmax and MSLP fit the pressure–wind relationship provided that aircraft observations are available. The aircraft data provide independent observations of Vmax and MSLP. When aircraft or other pertinent data are not available, the satellite intensity estimates along with a pressure–wind relationship are used to assign Vmax and MSLP, so that independent Vmax and MSLP are unavailable for the best-track data.

Defining the pressure–wind relationship for Vmax as a function of MSLP or vice versa gives a line of best fit to observations of each parameter. However, the degree to which best-track data agree with a pressure–wind relationship is mainly an indicator of whether or not independent observations of Vmax and MSLP were available. A more refined pressure–wind relationship would quantify not only the associated average or most likely value, but also the expected variability. Another way to refine the pressure–wind relationship is with

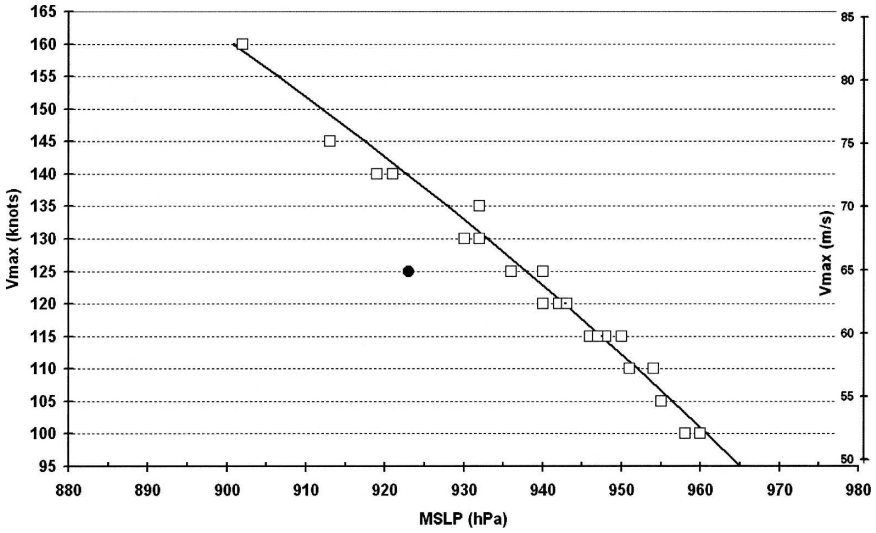

FIG. 7. Same as in Fig. 6, but for each 1995–2005 eastern Pacific major hurricane.

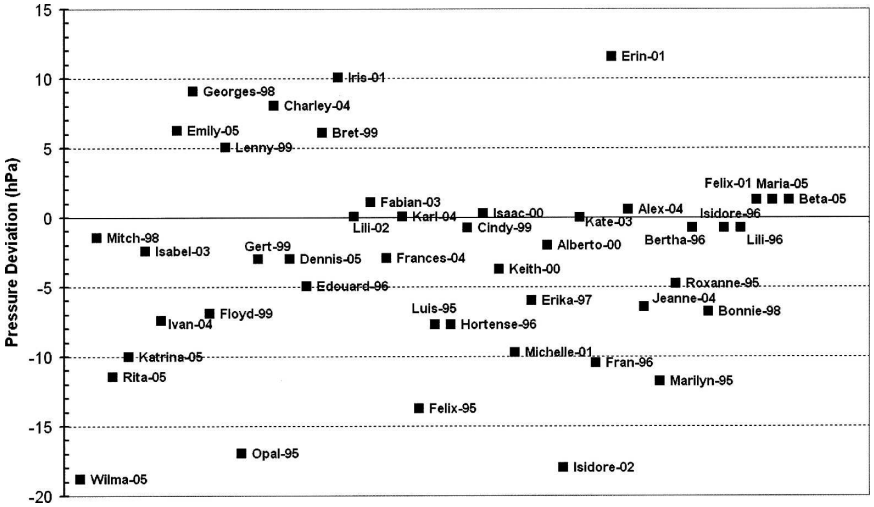

FIG. 8. Pressure deviations for each 1995–2005 Atlantic major hurricane according to the MSLP-observed minus the MSLP specified by Vmax and the Dvorak (1984) pressure–wind relationship. The lowest MSLP and highest Vmax from the best-track data (Figs. 4–6) are used. The points are plotted left to right in order of decreasing Vmax. The average is –3.1 hPa with a standard deviation of 7.1.

additional measurements. For example, defining a "delta-*p*" as environmental pressure (*p*-env) minus MSLP, allows the pressure–wind relationship to be expressed in terms of Vmax and delta-*p*, along with an observation of *p*-env.

To evaluate the pressure–wind relationship for the 45 1995–2005 Atlantic major hurricanes near the time of their maximum intensity, several steps were taken to obtain an improved dataset.

1) Vmax–MSLP pairs were used that have matching times in the best-track data. Some of the data in Figs. 6 and 8 are for Vmax and MSLP from the same hurricane but at different times.
2) Only Vmax–MSLP pairs are used that are based on aircraft observations.
3) Additional Vmax–MSLP pairs from the best track have been added using major hurricanes with multiple intensity maxima, or those that had clearly different pressure–wind relationships at different times. This results in a dataset of 52 Vmax–MSLP pairs.
4) An environmental pressure (*p*-env) was computed for each Vmax–MSLP pair. The relationship between hurricane wind speed and sea level pressure is described by simple conceptual and empirical models (Holland 1980). The environmental sea level pressure is used in those models, along with the MSLP, to parameterize the radial pressure gradient. It is likely best measured by averaging the pressure analysis over a broad ring surrounding the hurricane. For this study, environmental pressure (*p*-env) is defined as the average sea level pressure in the hurricane centered area with a radius of 800 to 1000 km. Reanalysis data (Kalnay et al. 1996) for the time of each Vmax–MSLP pair are used to compute *p*-env. Delta-*p* is defined as *p*-env minus MSLP.

Figure 9 is a plot of the pressure deviations with the 52 Vmax–MSLP pairs and it appears similar to Fig. 8. The average pressure deviation is –3.7 hPa with a standard deviation of 8.7, compared with −3.1 hPa and a standard deviation of 7.1 with the data in Fig. 8. There is a bit less agreement with the pressure–wind relationship with the Fig. 9 dataset, because Fig. 8 includes those 13 cases, for which no aircraft data were available.

The environmental pressure (*p*-env) with each Vmax–MSLP pair ranges from 1006.8 hPa with Hurricane Opal (1995) to 1021.6 hPa with Hurricane Erin (2001), and the average *p*-env is 1013.2 hPa. With Opal the low *p*-env of 1006.8 hPa partly explains its unusually negative deviation of MSLP from the pressure–wind relationship. Likewise, Erin's *p*-env of 1021.9 explains much of its anomalously high MSLP, given the Vmax.

Figure 10 is the corresponding plot of the 52 Vmax–MSLP pairs using delta-*p* instead of MSLP. The average pressure deviation of −3.7 hPa is reduced to −0.9 hPa by using delta-*p*. Table 3 lists the averages and standard deviations of the observed MSLP differences from pressure–wind relationship (Dvorak 1984) with the three datasets shown in Figs. 8–10.

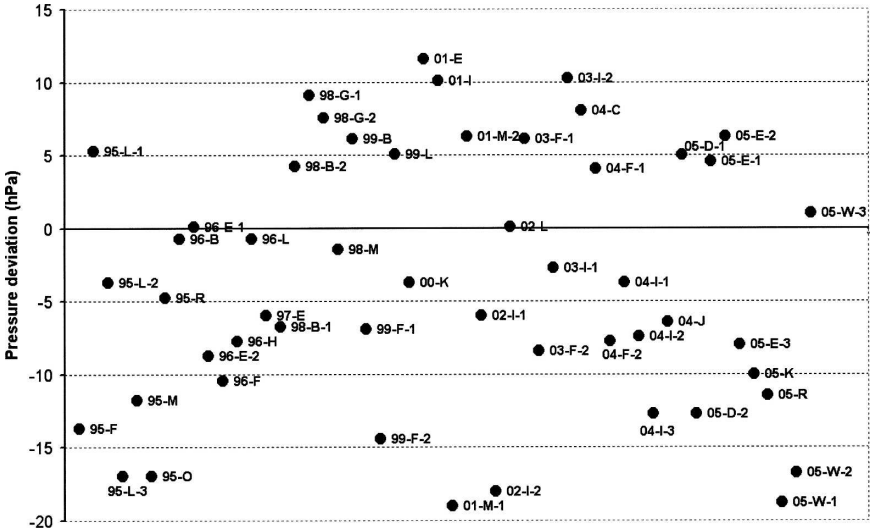

FIG. 9. Deviations of MSLP-observed and the MSLP specified by Vmax and the Dvorak (1984) pressure–wind relationship for the pressure–wind dataset of 52 cases. Each point is plotted in date–time order and labeled *yy-A-n*, where *yy* is the 2-digit year, *A* is the first letter of the hurricane name, and *n* is the number of data points from the same hurricane if there are more than one. The average pressure deviation is –3.7 hPa with a standard deviation of 8.7.

The Dvorak (1984) pressure–wind relationship used here and plotted in Figs. 6–7 is approximated by

$$\text{MSLP} = 1021.36 - 0.36(\text{Vmax}) - (\text{Vmax}/20.16)^2.$$

(MSLP in hPa and Vmax in kt).

This is a least squares fit to the pressure–wind table in Dvorak (1984). This relationship can be equivalently quantified as delta-*p*, using a *p*-env of 1016 hPa, following the method developed in Knaff and Zehr (2007):

$$\text{delta-}p = -5.36 + 0.36(\text{Vmax}) + (\text{Vmax}/20.16)^2.$$

This is used along with observed delta-*p* to compute the pressure deviations plotted in Fig. 10. The results in Fig. 9 indicate that the Dvorak (1984) pressure–wind relationship has a small bias (3.7 hPa) toward lower

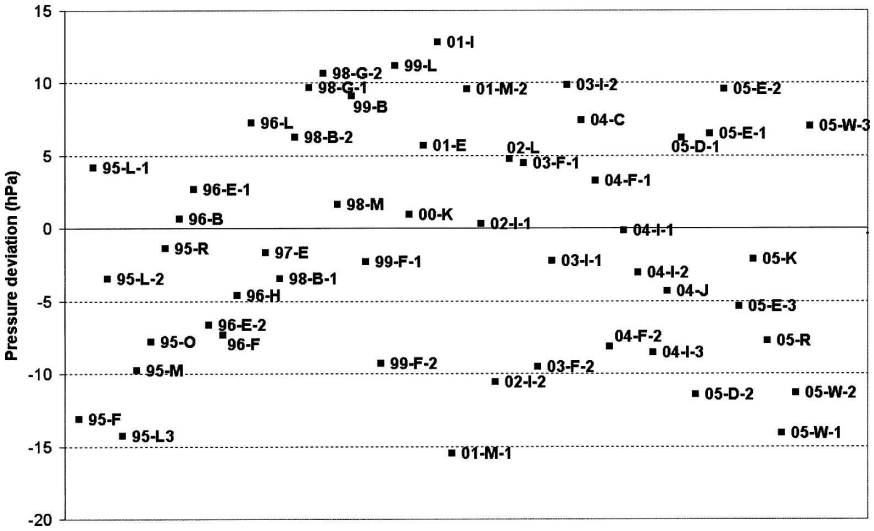

FIG. 10. Deviations of delta-*p*-observed and the delta-*p* specified by Vmax and the Dvorak (1984) pressure–wind relationship for the pressure–wind dataset of 52 cases. The average pressure deviation is –0.9 hPa with a standard deviation of 7.8.

TABLE 3. Averages and standard deviations of the pressure deviations from the pressure–wind relationship (Dvorak 1984), for 1995–2005 Atlantic major hurricanes (shown in Figs. 8–10).

Dataset	Average (hPa)	Std dev (hPa)
Lowest MSLP–highest Vmax 45 cases (see Fig. 8)	−3.1	7.1
MSLP–Vmax pairs 52 cases (see Fig. 9)	−3.7	8.7
Delta-p–Vmax pairs 52 cases (see Fig. 10)	−0.9	7.8

MSLP, when applied to this sample of major hurricanes. By using an observed *p*-env and a pressure–wind relationship expressed as a delta-*p*, this bias is reduced to 0.9 hPa; however, the scatter of the points is only slightly reduced (Table 3). The 2.8-hPa difference between the average pressure deviation in Figs. 9 and 10 (see Table 3) matches the difference between the Dvorak relationship's assumed *p*-env of 1016 hPa and the average observed *p*-env of 1013.2.

Erickson (1972) showed that different pressure–wind relationships were needed for the western North Pacific basin versus the Atlantic basin. Dvorak's subsequent publications (Dvorak 1975, 1984) recommended use of satellite intensity assignments along with pressure–wind relationships for both the Atlantic and western North Pacific. Harper (2002) discusses the influence of the lower climatological environmental pressure in the western North Pacific on the differences in pressure–wind relationships. Documentation on the operational use of pressure–wind relationships can be found in Guard et al. (1992), Harper (2002), and Velden et al. (2006).

e. Other influences on the pressure–wind relationship

Weatherford and Gray (1988) showed that tropical cyclone size as measured by the radial extent of gale force winds is highly variable for a given intensity. This is also true for Atlantic major hurricanes, as will be shown in section 10. Hurricanes Bret (1999), Iris (2001), and Charley (2004) were small hurricanes. Their cloud shields and extent of circulation were distinctly smaller than average. In Fig. 10 all of those three small hurricanes (denoted 99-B, 01-I, and 04-C) have delta-*p* smaller (MSLP higher) than what is indicated by applying the pressure–wind relationship to their Vmax. This indicates that a different pressure–wind relationship is likely warranted for small hurricanes. These findings are similar to Guard and Lander (1996) for western North Pacific midget tropical cyclones (TCs) and Love and Murphy (1985) for the subset of Australian northern region storms, which tend to be smaller than average.

A much larger data sample is needed to thoroughly investigate pressure–wind relationships and identify the influences on Vmax and MSLP. Knaff and Zehr (2007) show that an improved pressure–wind relationship can be derived using a large sample and some additional measurements. Their results use observations of location (latitude), environmental pressure, storm translation speed, and size to get improved estimates of MSLP from the Vmax and vice versa, over a wide range of intensity.

6. Major hurricane duration

The best-track data provide a measurement of the duration of 100 kt (51.4 m s^{-1}) or greater intensity in increments of 0.25 days (6 h), plotted in Fig. 11 for 1995–2005 Atlantic major hurricanes. While Hurricane Opal (1995) ranks as seventh most intense in terms of its MSLP (916 hPa), it is a very modest 31st in rank according to major hurricane duration. Hurricane Ivan (2004) had the maximum number of major hurricane days with 10.0, while the average for the 45 cases is 2.7.

The major hurricane duration is influenced by the storm track in addition to the favorable conditions for intensification. Obviously, those that become major hurricanes at lower latitude and in the eastern Atlantic away from large landmasses are more likely to have tracks that remain longer over warm ocean areas, and therefore a better chance to persist as a major hurricane.

7. Intensification rate

a. Best track: 24-h period

It is important to know the rate at which hurricanes can intensify. The standard best track times of 0000, 0600, 1200, and 1800 UTC are used to compute two intensity change quantities, –dMSLP-24, the 24-h decrease of MSLP, and dVmax-24, the 24-h increase in maximum wind speed. The greatest intensification rates for each hurricane are plotted in Figs. 12 and 13. The average maximum intensification rates for the 1995–2005 Atlantic major hurricanes are 34.2 hPa day^{-1} and 41 kt day^{-1} (21.1 m s^{-1} day^{-1}), while the extreme values are 97 hPa day^{-1} and 95 kt day^{-1} (48.8 m s^{-1} day^{-1}) with Hurricane Wilma (2005). A more extensive study of Atlantic tropical cyclone intensification rates by Kaplan and DeMaria (2003) documented that "rapid

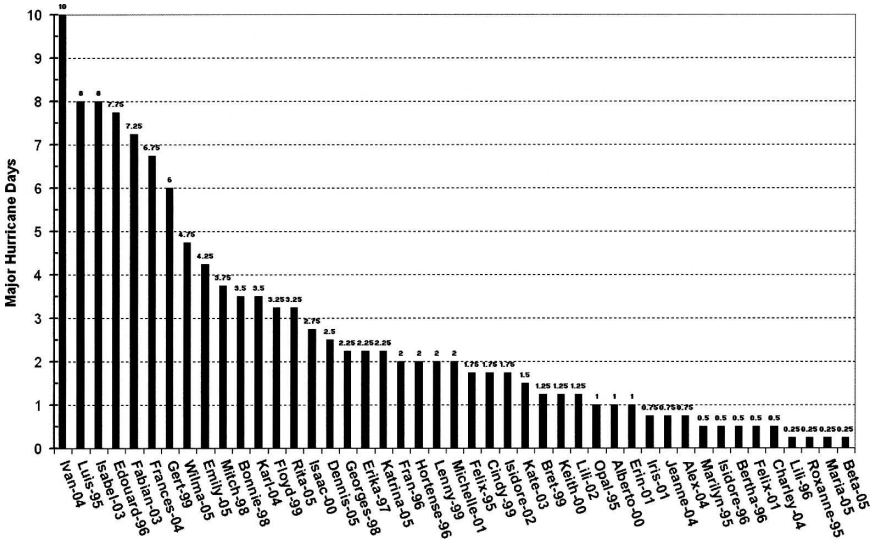

FIG. 11. Major hurricane duration (IH-Days) for each 1995–2005 Atlantic major hurricane, using best-track data. The IH-Days average is 2.7 with a standard deviation of 2.5.

intensification" defined by the 95th percentile of all observed intensity changes, is associated with 83% of major hurricanes and all hurricanes of Saffir–Simpson category 4 or 5. The 95th percentile rate for dVmax-24 from the Kaplan and DeMaria (2003) study is 31 kt day^{-1} (16.0 m s^{-1} day^{-1}). Similar results are found with the maximum intensification rates of the 1995–2005 major hurricanes, plotted in Fig. 13. Sixty-nine percent have dVmax-24 of at least 35 kt day^{-1} (18.0 ms^{-1} day^{-1}) and 91% are at least 30 kt day^{-1} (15.4 m s^{-1} day^{-1}), which is the Kaplan and DeMaria (2003) threshold for "rapid intensification." Of the 28 hurricanes that are category 4 or higher, all of the maximum intensification rates are at least 25 hPa day^{-1} and 30 kt day^{-1} (15.4 m s^{-1} day^{-1}).

b. *Aircraft center fixes: 12-h period*

Aircraft reconnaissance center fix sea level pressure (MSLP) observations provide additional insight on intensification rates due to the reliability of more direct measurements and typical observation intervals less

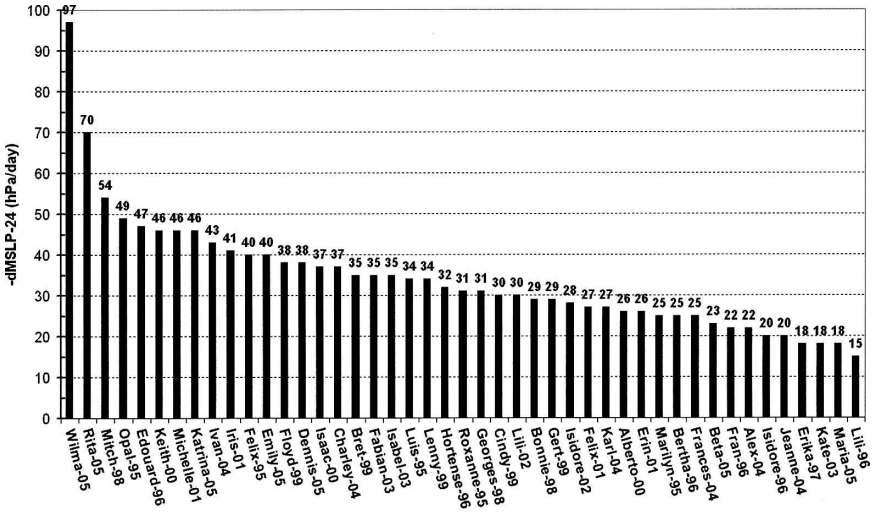

FIG. 12. Highest intensification rate according to 24-h change of MSLP (−dMSLP-24) for each 1995–2005 Atlantic major hurricane, using best-track data. The average −dMSLP-24 is 34.2 hPa with a standard deviation of 14.5.

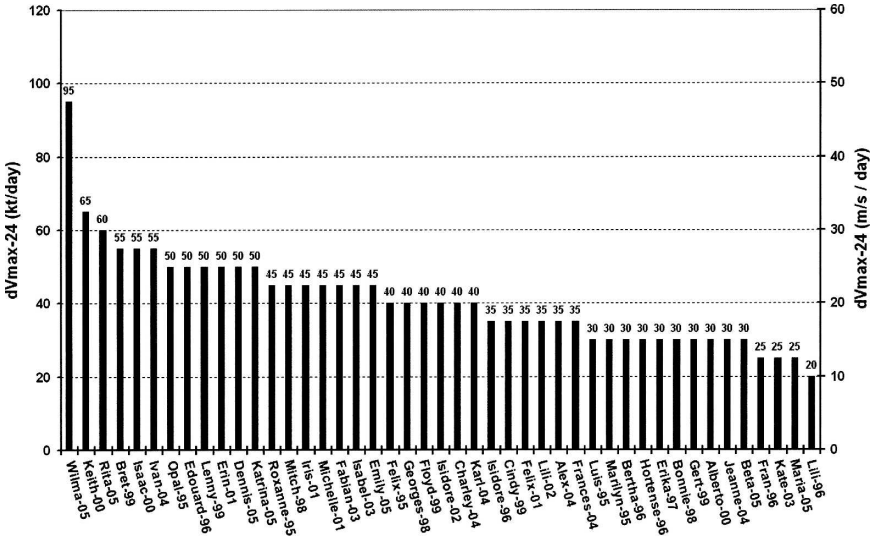

FIG. 13. Highest intensification rate according to 24-h change of Vmax (dVmax−24) for each 1995–2005 Atlantic major hurricane using best-track data. The average dVmax−24 is 41.0 kt day^{-1} (21.1 m s^{-1} day^{-1}) with a standard deviation of 13.2 (6.8).

than 6 h. With the 1995–2005 category 4–5 Atlantic hurricanes, 18 had intensification periods that were well observed by aircraft. The largest 12-h MSLP decreases using linear interpolation with available aircraft observations (−dMSLP-12) are plotted in Fig. 14. The 12-h interval generally results in faster intensification rates than the 24-h computations. The average of the 18 cases was 63.4 hPa day^{-1}, with a median value of 54 hPa day^{-1}, while Hurricane Wilma (2005) had a remarkable 175 hPa day^{-1} intensification rate over a 12-h period. Using the 6-h fixed time intervals of the best-track data, Wilma's maximum 12-h MSLP decrease is 83 hPa (166 hPa day^{-1}). The Tropical Prediction Center's Tropical Cyclone Report on Wilma (Pasch et al. 2006) has a discussion of this record breaking intensification rate, and they note that over a shorter period, an intensification rate of 9.9 hPa h^{-1} (237.6 hPa day^{-1}) was recorded.

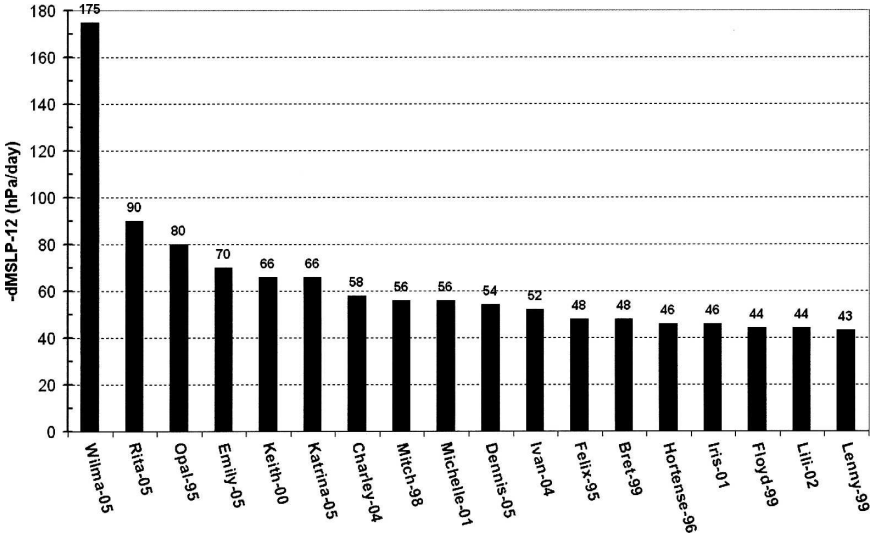

FIG. 14. Highest intensification rate according to 12-h change of aircraft observations of MSLP (−dMSLP-12) for the 1995–2005 Atlantic category 4–5 hurricanes. The average –dMSLP-12 is 63.4 hPa day^{-1} with a standard deviation of 30.8.

8. Storm motion

The velocity of the hurricane center location is referred to as the "storm motion." The storm motions at the time of maximum intensity for the 1995–2005 Atlantic major hurricanes were compiled from the Tropical Prediction Center Advisories when available and alternatively from the 6-h best-track positions. The storm motion vectors are listed in Table 4. The average vector is toward 325 degrees at 5.8 m s^{-1} (11.3 kt), indicating that on average major hurricanes attain maximum intensity prior to recurvature. However, the main feature of this storm motion dataset is the high variability. The standard deviation of storm motion speed is 2.4 m s^{-1} (4.7 kt). In fact, 11 of the 45 cases have a northeastward component of motion at maximum intensity. The speed of motion ranged from zero (i.e., nearly stationary) with Hurricane Keith (2000) to 11.5 m s^{-1} (22 kt) with Hurricanes Lili (1996) and Alex (2004).

TABLE 4. Storm motion directions and speeds in m s^{-1} and kt, at the time of maximum intensity. Directions are in degrees of direction toward which the hurricane center is moving. The average direction and speed is toward 325 degrees at 5.8 m s^{-1} (11.3 kt), with a standard deviation of 2.4 m s^{-1} (4.7 kt).

Name (year)	Direction	Speed (ms^{-1})	Speed (kt)
Felix (1995)	310	5.7	11
Luis (1995)	335	8.2	16
Marily (1995)	330	5.1	10
Opal (1995)	35	8.2	16
Roxanne (1995)	275	4.6	9
Bertha (1996)	305	8.7	17
Edouard (1996)	295	6.2	12
Fran (1996)	335	5.7	11
Hortense (1996)	10	6.7	13
Isidore (1996)	325	5.7	11
Lili (1996)	65	11.3	22
Erika (1997)	25	6.7	13
Bonnie (1998)	325	2.6	5
Georges (1998)	280	7.7	15
Mitch (1998)	290	3.6	7
Bret (1999)	315	4.6	9
Cindy (1999)	335	4.1	8
Floyd (1999)	275	5.1	10
Gert (1999)	275	4.6	9
Lenny (1999)	50	4.1	8
Alberto (2000)	75	8.2	16
Isaac (2000)	315	7.7	15
Keith (2000)	0	0	0
Erin (2001)	330	5.7	11
Felix (2001)	50	6.2	12
Iris (2001)	260	8.2	16
Michelle (2001)	10	1.5	3
Isidore (2002)	255	3.6	7
Lili (2002)	315	7.2	14
Fabian (2003)	330	4.1	8
Isabel (2003)	270	4.1	8
Kate (2003)	280	5.1	10
Alex (2004)	65	11.3	22
Charley (2004)	15	9.8	19
Frances (2004)	285	7.7	15
Ivan (2004)	285	3.6	7
Jeanne (2004)	280	5.7	11
Karl (2004)	340	5.1	10
Dennis (2005)	340	8.2	16
Emily (2005)	295	8.2	16
Katrina (2005)	315	5.7	11
Maria (2005)	020	3.1	6
Rita (2005)	280	4.1	8
Wilma (2005)	300	3.1	6
Beta (2005)	245	3.6	7

9. IR image measurements

a. Digital Dvorak technique

Dvorak (1984) proposed a method for estimating intensity based on IR pixel temperatures. The same method has been applied to 30-min interval IR images with all forty-five 1995–2005 Atlantic major hurricanes, except that multiple radius measurements of the surrounding temperature were employed. For major hurricanes, the algorithm is very similar to the Objective Dvorak Technique (ODT) described in Velden et al. (1998), and the Advanced Objective Dvorak Technique (Olander and Velden 2004, 2007).

The digital Dvorak intensity estimates are shown in Fig. 15 as T-No.-6 (the maximum 6-h running mean of the Dvorak intensity) and in Fig. 16a as T-max (the maximum single image Dvorak intensity number). The digital Dvorak intensities (T-numbers) are specified to the nearest 0.1. Table 5 lists the T-number conversion to maximum surface wind speed for the range of values in Figs. 15–16. The T-No.-6 values ranged from a high of T7.6 with Hurricane Wilma (2005) to a low of T5.6 with Hurricane Felix (2001), averaging T6.6 for all 1995–2005 Atlantic major hurricanes.

The IR measurements comprising the objective intensity estimates are plotted in Fig. 16 and summarized in Table 6. Surr-T is the "surrounding temperature" defined as the warmest IR pixel temperature on the coldest circle, and it ranges from –58.2° to –81.2°C, averaging –71.3°C. The Eye-T is the warmest IR pixel temperature in the eye. Cloud-free eyes have temperatures in the 15°–20°C range, a few degrees cooler than the ocean surface due to water vapor attenuation. The average Eye-T is 1.0°C with a median value of 10.8°C. There is a large eye temperature range from 20.3°C with Hurricane Rita (2005) to −65.2°C with Hurricane Beta (2005). Eye temperatures in the 0°–15°C range are typically observed with low-level clouds within the eye. A few major hurricanes have colder Eye-T values. With

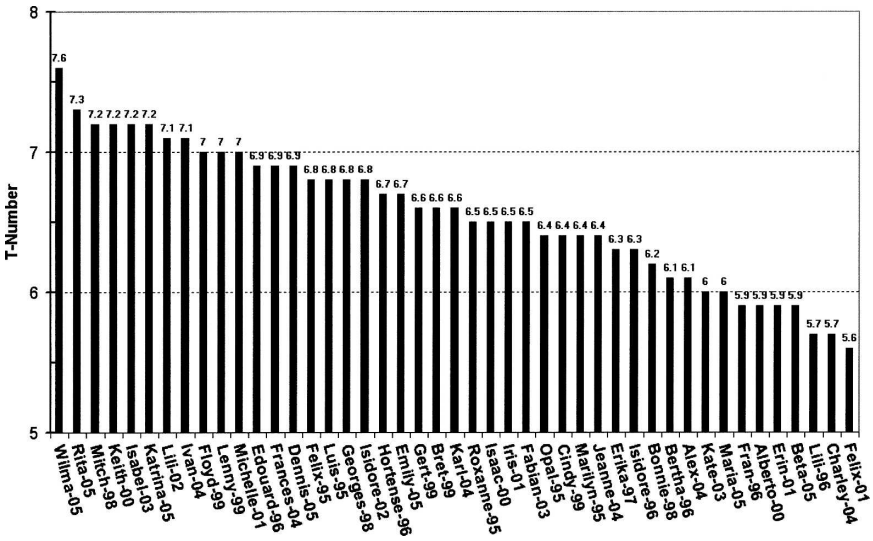

FIG. 15. Digital Dvorak technique maximum intensity (T-No.-6) for each 1995–2005 Atlantic major hurricane. The 6-h running mean of T numbers is used. The average T-No.-6 is 6.6 with a standard deviation of 0.5.

weaker hurricanes, this is commonly observed, with high clouds covering the eye. However, with major hurricanes it may also be due to a very small eye or poor viewing angle, limiting the capability of the IR sensor to view directly down to the low levels, as with Hurricanes Opal (1995), Charley (2004), and Wilma (2005). With Hurricane Beta, the eye was both very small and partly cloud covered.

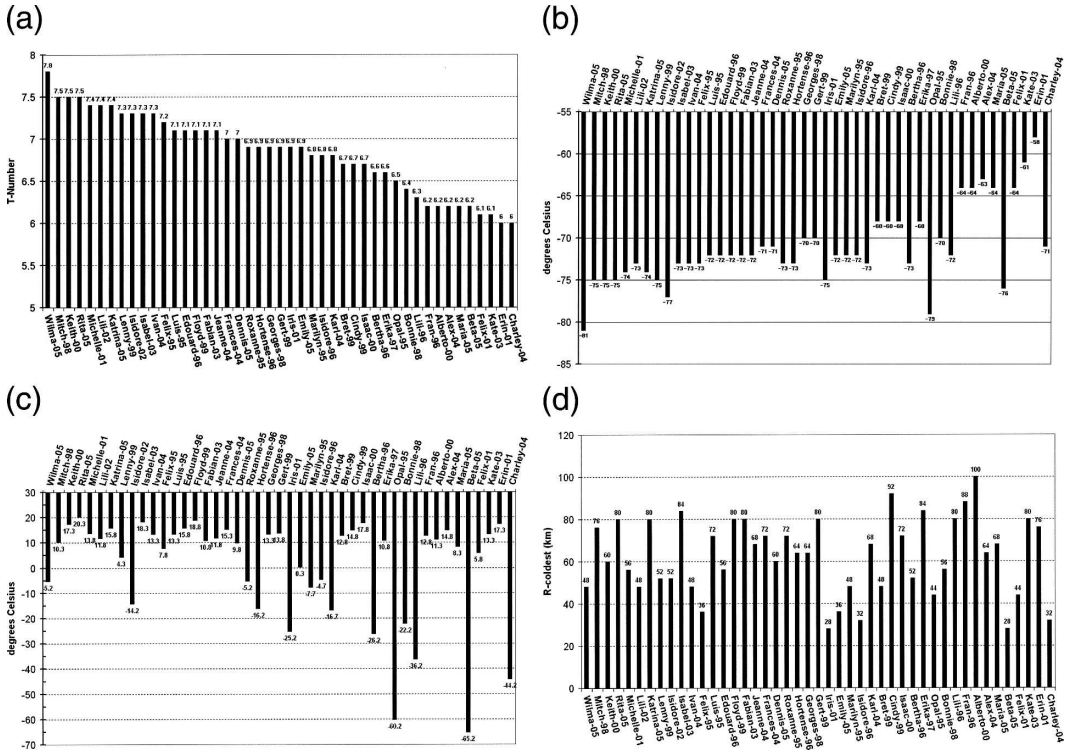

FIG. 16. Digital Dvorak technique associated measurements. (a) Single image maximum (T-max). (b) Surrounding temperature (°C) (Surr-T). (c) Eye temperature (°C) (Eye-T). (d) Radius (km) of coldest Surr-T (R-coldest).

TABLE 5. Conversion of Dvorak T-No. to maximum surface wind speed.

T-No.	Max wind speed ($m\ s^{-1}$)	Max wind speed (kt)
5.5	52.4	102
6.0	59.1	115
6.5	65.3	127
7.0	71.9	140
7.5	79.7	155
8.0	87.4	170

TABLE 6. IR measurements with digital Dvorak technique for the single image maximum (T-max). Average, standard deviation, maximum, minimum for T-max, Surr-T, Eye-T, and R-coldest.

	T-max	Surr-T (°C)	Eye-T (°C)	R-coldest (km)
Average	6.8	−71.3	1.0	62.4
Standard deviation	0.47	4.6	21.0	18.3
Maximum	7.8	−58.2	20.3	100
Minimum	6.0	−81.2	−65.2	28

Here R-coldest is the radius of the circle with the coldest temperatures, as defined by the "surrounding temperature." The R-coldest radii are given in increments of 4 km corresponding to the approximate resolution of the IR sensor. The inner radius is assigned as R-coldest when multiple radii have the same surrounding temperature. R-coldest averaged 62.4 km, with a broad range from 28 km for Hurricane Iris (2001), a very small hurricane, to 100 km for Hurricane Alberto (2000), which had a large eye. Data are shown in section 10 relating R-coldest and the radius of maximum wind.

The digital Dvorak intensities are compared with best-track Vmax in Fig. 17, according to the overall maximum for the entire hurricane period. In Fig. 18, the digital Dvorak intensity is converted to MSLP according to the Dvorak (1984) pressure–wind relationship and plotted against the best-track MSLP interpolated to the same time as the digtial Dvorak maximum. Both Figs. 17 and 18 include the 13 cases for which intensity was analyzed without aircraft observations. There is a general tendency for the digital Dvorak to give intensities that are stronger (lower MSLP) than the best track. However, with several notable hurricanes, it indicates less intense hurricanes than the best track. Hurricane Charley (2004) with respect to Vmax (Fig. 17), and Hurricanes Opal (1995) and Wilma (2005) with MSLP (Fig. 18) have the largest digital Dvorak underestimates of maximum intensity. The underestimates with Opal, Charley, and Wilma are likely due to the small eyes and resulting colder-than-average eye temperatures, as previously discussed.

With Hurricane Opal (1995), the maximum intensity from the digital Dvorak technique converted to MSLP is 938 hPa, considerably less intense than the best-track MSLP of 916 hPa. However, in terms of Vmax, the satellite intensity estimate is only 2.6 $m\ s^{-1}$ (5 kt) less than the best track Vmax of 66.8 ms^{-1} (130 kt). This shows that validation of the digital Dvorak technique with Vmax versus MSLP can give different results when large deviations from the Dvorak (1984) pressure–wind relationship are observed.

Hurricanes Keith (2000) and Michelle (2001) have digital Dvorak estimates exceeding the best-track maximum by at least 10.3 $m\ s^{-1}$ (20 kt). It is interesting to note that these were unusually slow-moving hurricanes (Table 4), and that the satellite algorithm does not account for variations of storm motion but assumes a sample mean value.

A more thorough validation of the digital Dvorak technique and the ODT is given by Velden et al. (1998). The differences between the satellite-derived and best-track intensities shown in Figs. 17–18 suggest a high bias in the digital Dvorak technique's intensities (low bias in MSLP estimates). It is more pronounced with category 3 hurricanes and becomes less with higher intensities. This characteristic merits further investigation to see if it is present in an expanded dataset. A credible evaluation of the performance and accuracy of the digital Dvorak and the ODT requires a greatly expanded dataset using both MSLP and Vmax, with cases that are well observed by aircraft.

b. IR cold cloud areas

Along with the digital Dvorak IR temperatures, the images can be further quantified by computing the percent area coverage of pixels colder than a threshold temperature, which give a measure of the amount and intensity of deep convection. Figure 19 shows the areal coverage of IR cloud colder than –60°C within 4 degrees latitude (444 km) of the center, which averages 24.3% and ranges from a maximum of 58.2% for Hurricane Wilma (2005) to a 5.7% minimum for Hurricane Erin (2001). With a –70°C temperature and a 2-degrees-latitude (222 km) radius (Fig. 20), the percent coverage averages 29% with a maximum of 87.9% for Wilma.

Even though there is a small tendency for more major hurricanes to have larger IR cold cloud areas, large differences are observed with a few hurricanes of comparable intensity. Some category 4 hurricanes [Hurricanes Iris (2001), Bret (1999), and Charley (2004)] have small cold cloud areas while weaker hurricanes have larger cold cloud areas. For example, Hurricane Isidore (2002) with a Vmax of 110 kt (57 $m\ s^{-1}$) ranked seventh

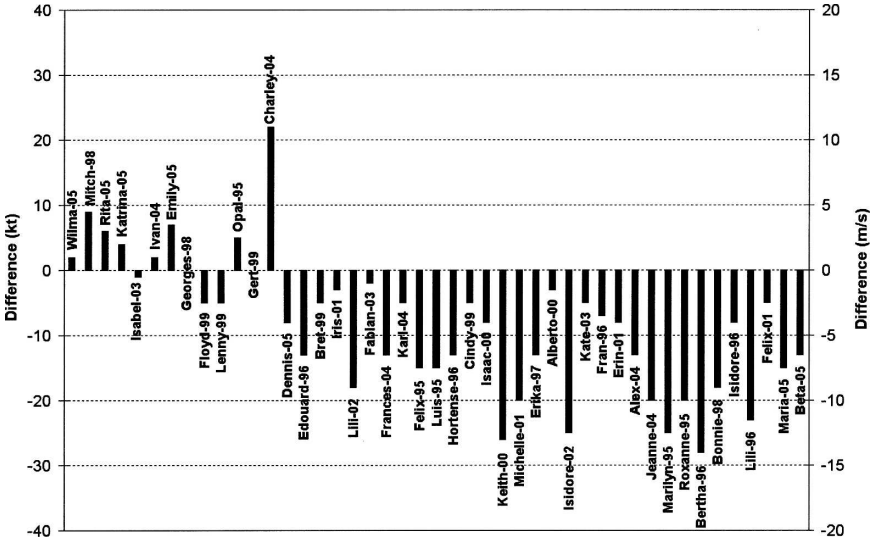

FIG. 17. Best track minus digital Dvorak technique maximum intensity according to the highest Vmax in the best track and the hurricane maximum digital Dvorak (Fig. 15). Wind speed differences are plotted left to right in order of intensity given by highest Vmax (Fig. 4). Positive values indicate the digital Dvorak underestimates Vmax compared with the best track, and negative values are overestimates.

with 36.7% of the 0–444-km area colder than –60°C, while Hurricane Charley at 130 kt (67 m s^{-1}) has only 12.6% coverage. Several category 3 hurricanes [Hurricanes Roxanne (1995), Bertha (1996), Erika (1997), and Bonnie (1998)] have above-average cloud area colder than –60°C. Much of this IR cloud area variability is clearly related to hurricane size, which is discussed along with wind radii measurements next in section 10.

10. Wind radii and size

a. R-34 and R-50

Several different parameters have been used to indicate hurricane size. The outer closed isobar of the sea level pressure analysis, the zero line of cyclonic tangential wind, and various surface wind isotachs all vary according to the radial extent of the hurricane's surface

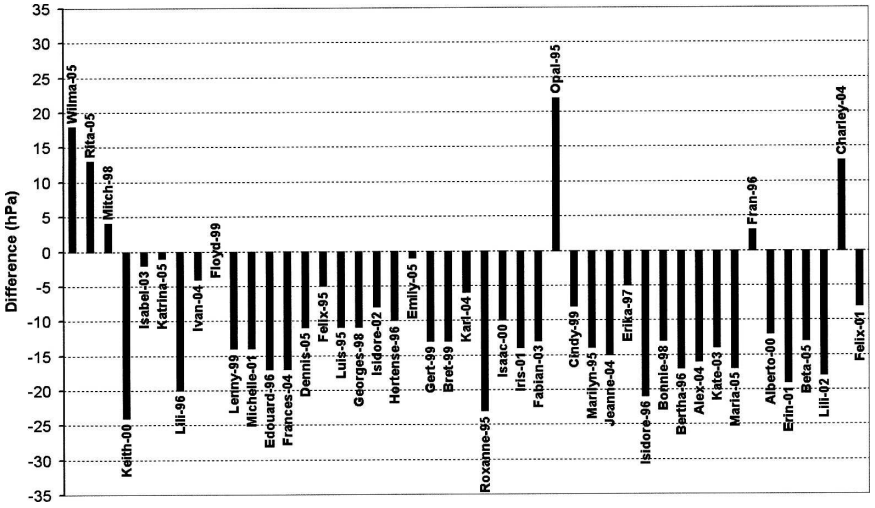

FIG. 18. Digital Dvorak technique minus best-track maximum intensity, according to MSLP interpolated to time of maximum intensity using the digital Dvorak. The differences are plotted left to right in order of digital Dvorak intensity (Fig. 15). Positive values indicate that digital Dvorak is underestimating intensity (too high MSLP) compared with the best track and negative values are overestimates (too low MSLP).

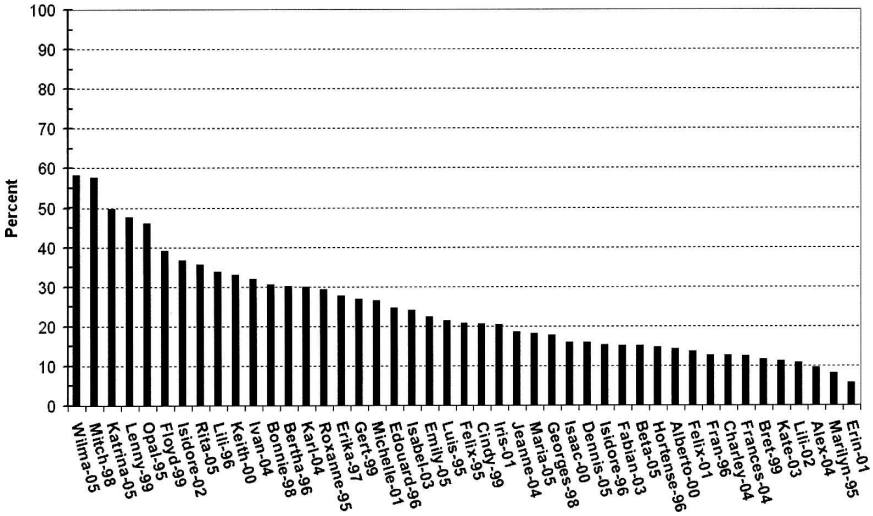

FIG. 19. Percent of IR pixels $<-60°C$ within 444 km of center, for each 1995–2005 Atlantic major hurricane, at the time of their maximum intensity, according to lowest MSLP. The average is 24.3% with a standard deviation of 13.0.

circulation. Tropical cyclone size is not well related to intensity and the size often continues to increase following the time of maximum intensity (Weatherford and Gray 1988; Maclay 2006). The advisories issued by the Tropical Prediction Center include estimates of the radial extent of winds greater than 34 (17.5 m s^{-1}) (R-34) and 50 kt (25.7 m s^{-1}) (R-50) in quadrants. The quadrant values were averaged at the best-track time of maximum intensity for the forty-five 1995–2005 Atlantic major hurricanes and are plotted in Fig. 21 (R-34) and Fig. 22 (R-50). High variability and large ranges are shown by the wind radii.

The size differences that can occur among major hurricanes are shown by comparing the wind radii values of large hurricanes [Hurricanes Luis (1995), Cindy (1999), and Erika (1997)] with the small values associated with Hurricanes Iris (2001), Bret (1999), Charley (2004), and Beta (2005). R-34 ranges from 427 km with Cindy (1999) to 93 km with Beta. R-50 ranges from 278 km with Luis to 43 km with Iris. The averages and standard deviations of R-50 and R-34 at maximum intensity are listed in Table 7 along with the radius of maximum wind (RMW), which is discussed in the next section.

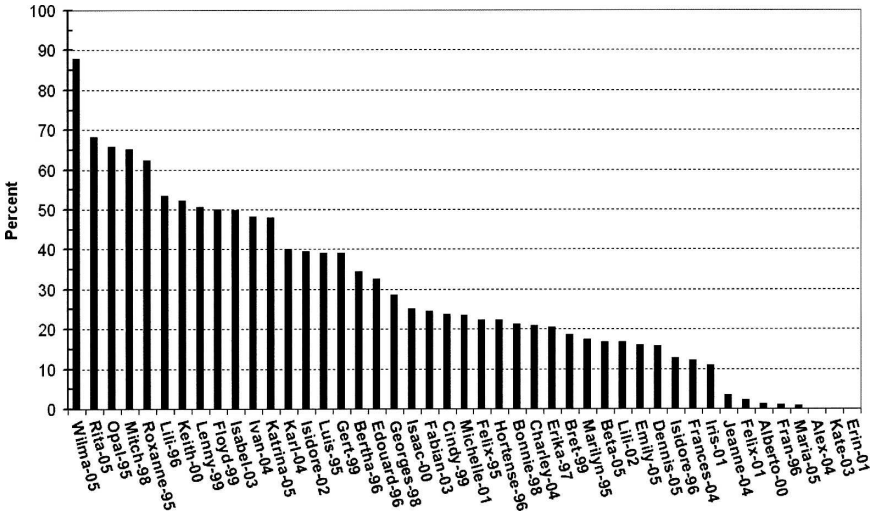

FIG. 20. Percent of IR pixels $<-70°C$ within 222 km of center, for each 1995–2005 Atlantic major hurricane, at the time of their maximum intensity, according to lowest MSLP. The average is 29.0% with a standard deviation of 20.0.

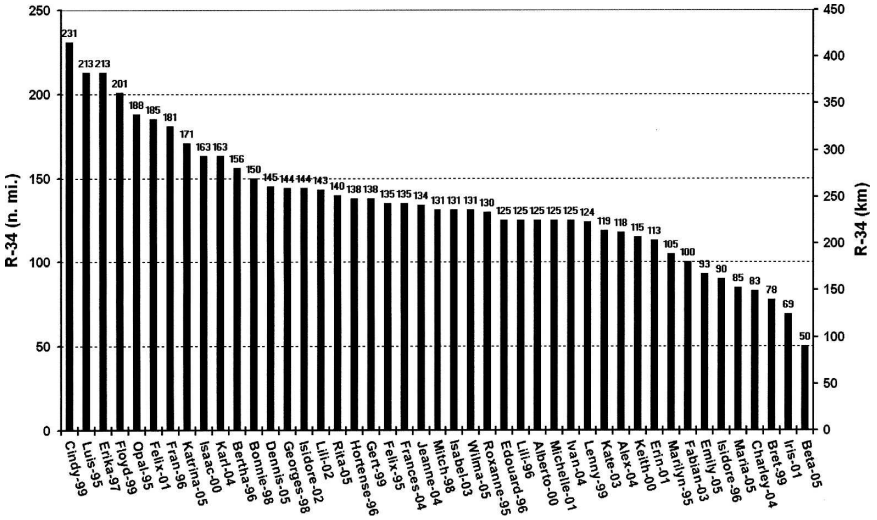

FIG. 21. Azimuthal average of the radius of 34-kt (17.5 m s^{-1}) wind speed (R-34), for each 1995–2005 Atlantic major hurricane, at the time of their maximum intensity, according to lowest MSLP. The average is 250.8 km (135.6 n mi) with a standard deviation of 71.1 km (38.5 n mi).

b. RMW

Estimates of the RMWs based on aircraft radar, aircraft flight level winds, and satellite images are included in the Tropical Prediction Center Advisory archives. The RMW at the time of best-track maximum intensity are shown in Fig. 23. The average value of 31.7 km has an associated standard deviation of 14.4 km (Table 7). Large hurricanes have a tendency toward greater RMW and vice versa; however, RMW and size are not closely related. For example, category 5 Hurricanes Mitch (1998) and Isabel (2003) both have near-average R-34 and R-50 (Figs. 21–22) but have very different corresponding RMWs (13 km for Mitch and 56 km for Isabel).

Along with Hurricane Wilma's (2005) record low MSLP and record intensification rates, an unusually small eye and associated RMW were observed (Pasch et al. 2006). Based on the aircraft center fix observations and the discussion of Pasch et al. (2006), Wilma's

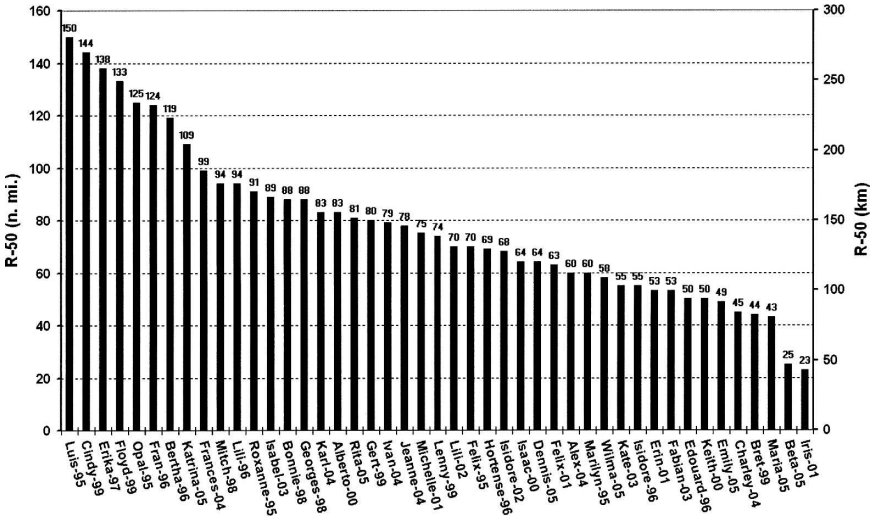

FIG. 22. Azimuthal average of the radius of 50-kt (25.7 m s^{-1}) wind speed (R-50), for each 1995–2005 Atlantic major hurricane, at the time of their maximum intensity, according to lowest MSLP. The average is 144.3 km (78.0 n mi) with a standard deviation of 56.2 km (30.4 n mi).

TABLE 7. Quadrant average radius of winds greater than 34 kt (17.5 m s^{-1}) (R-34), greater than 50 kt (25.7 m s^{-1}) (R-50), and the RMW for the 1995–2005 Atlantic major hurricanes at the time of maximum intensity. Average, std dev, maximum, and minimum values.

	R-34 (km)	R-50 (km)	RMW (km)	R-34 (n mi)	R-50 (n mi)	RMW (n mi)
Average	250.8	144.3	33.0	135.6	78.0	17.0
Std dev	71.2	56.2	15.6	38.5	30.4	8.0
Max	427	278	58.4	231	150	30
Min	93	42.5	3.9	50	23	2

RMW at maximum intensity is assigned 3.7 km (2.0 n mi), the minimum observed RMW of the 1995–2005 Atlantic major hurricanes (Fig. 23 and Table 7).

The RMW seems to be more variable than size and typically changes on shorter time scales. The phenomena of multiple wind maxima and eyewall cycles have been observed and documented (Willoughby et al. 1982). Hawkins et al. (2006) show that microwave images provide much-improved views of multiple eyewall configurations, compared with IR images.

c. *Relationships between wind radii and IR measurements*

Figure 24 is a scatterplot of the IR cold cloud areas from Fig. 19 and the R-34 in Fig. 21. It shows some correlation ($r = 0.26$) between the two quantities, however much of the variability remains unexplained. Some of this may be due to the data not necessarily being recorded at the same time; nevertheless an expanded dataset is needed to explore the relationship between IR cloud areas and size.

As discussed in section 9a, R-coldest is the radius of the circle with the coldest surrounding temperature. The RMW is plotted versus R-coldest in Fig. 25. There is a small correlation between the quantities ($r = 0.44$), with R-coldest being observed outside the RMW. The larger radius with the coldest IR ring is likely due to both an outward tilt of the eyewall and also some outward radial flow at the cloud top.

11. Landfalls

Loss of life and property damage is closely related to hurricane intensity at time of landfall. The landfall intensities from the Tropical Prediction Center archives for the 1995–2005 Atlantic major hurricanes are listed in Table 8 according to maximum surface wind speed. The date/time, MSLP, and location are also listed, including the multiple landfalls that occur with some hurricanes. Only landfalls of at least hurricane intensity that attained category 3 status at some point are included in the table.

Thirty-two of the forty-five 1995–2005 Atlantic major hurricanes (71%) made 58 landfalls with at least hurricane intensity. Thirty-five of those (60%) were major hurricanes (category 3 or greater) at landfall. Eleven of the 35 were (31%) were U.S. landfalls. The seven most intense 1995–2005 U.S. landfalls all occurred in 2004–05.

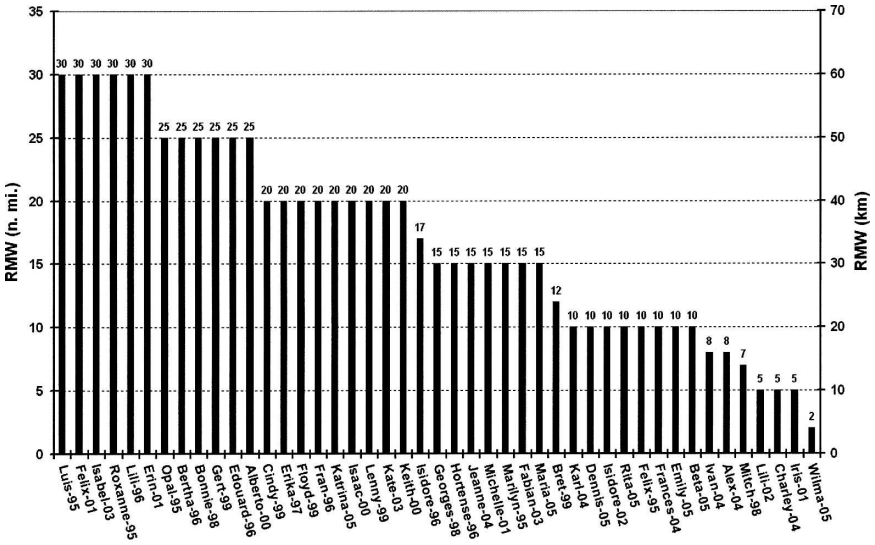

FIG. 23. RMW for each 1995–2005 Atlantic major hurricane, at the time of their maximum intensity, according to lowest MSLP. The average is 33.0 km (17.0 n mi) with a standard deviation of 15.6 km (8.0 n mi).

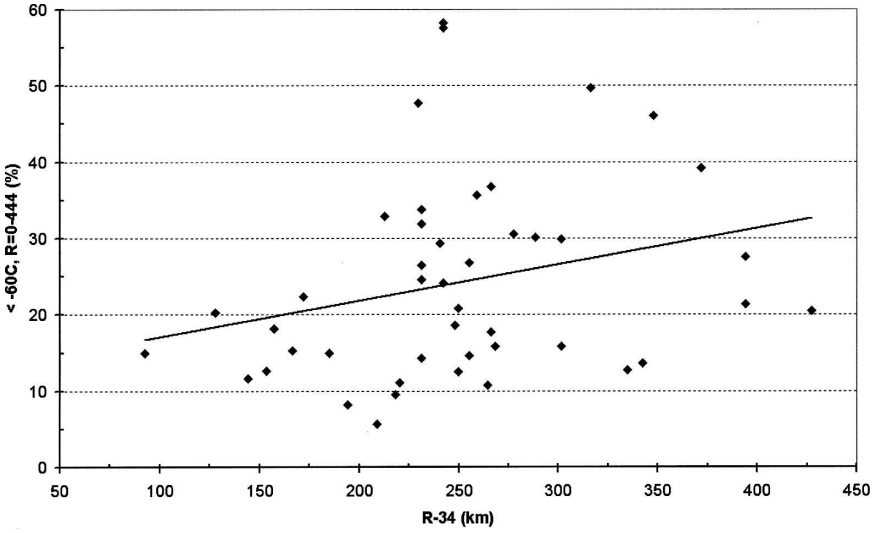

FIG. 24. Scatterplot of the average radius of 34 kt (17.5 m s^{-1}) wind speed (R-34), from Fig. 21, vs percent of IR pixels $<-60°C$ within 444 km of center, from Fig. 19. The least squares best-fit trend line is shown. Correlation coefficient: $r = 0.26$.

12. The 2005 Atlantic hurricane season

The Atlantic hurricane activity in 2005 was extraordinary. In terms of major hurricanes, there were seven (Fig. 2): four category 5, one category 4, and two category 3 hurricanes. Five of the 12 most intense 1995–2005 hurricanes according to MSLP (Fig. 5) occurred in 2005, and three of the five lowest MSLP since 1950 (Hurricanes Wilma, Rita, and Katrina) were in 2005. The 24-h MSLP decreases of Rita and Wilma (Fig. 12) exceeded all other 1995–2005 major hurricanes. In fact, Wilma's 24-h best-track decrease of MSLP of 97 hPa is remarkably large, compared with the median value for the 1995–2005 Atlantic major hurricanes of 32 hPa. Thirteen of the 58 landfalls listed in Table 7 were from 2005, including the devastating impacts of Hurricane Katrina in Louisiana and Mississippi.

13. Discussion

The best-track, aircraft, and IR satellite datasets provide an overview of the average and extreme measure-

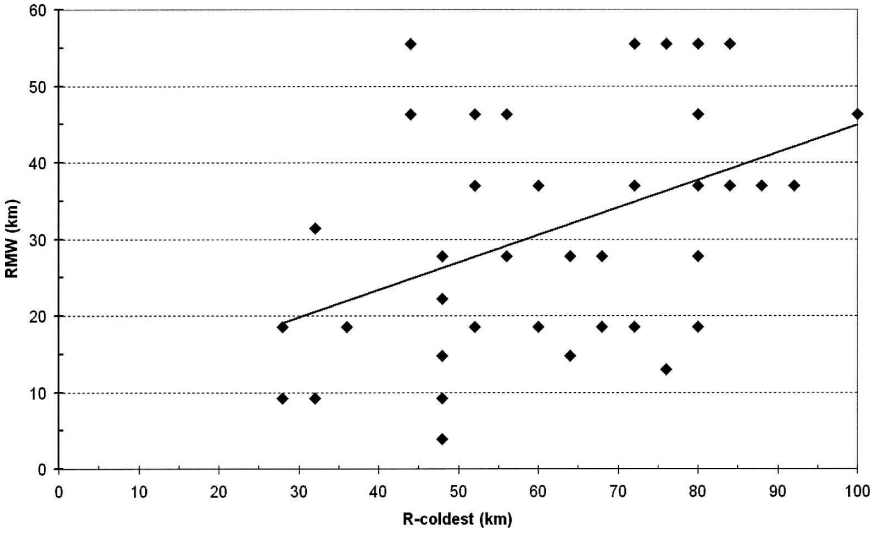

FIG. 25. Scatterplot of radius of coldest Surr-T (R-coldest) vs R-coldest vs RMW for each 1995–2005 Atlantic major hurricane, at the time of their maximum intensity. Correlation coefficient: $r = 0.44$.

TABLE 8. Landfall intensity for 1995–2005 Atlantic major hurricanes that were at least hurricane intensity at landfall, with date/time (UTC) as mm/dd/hh. Locations are given as Caribbean countries, and U.S./Mexico towns. The number in parentheses is the landfall number for hurricanes with multiple landfalls. "Closest approach" intensities are included when the center is within 25 n mi (46 km) of a coastline.

Hurricane	Max wind (kt)	MSLP (hPa)	Date/time	Location
1) Ivan (4)	140	916	9/14/0100	Cuba
2) Lenny	135	933	11/17/1800	U.S. Virgin Islands
3) Ivan (2)	130	924	9/11/0400	Jamaica
4) Ivan (3)	130	920	9/12/0400	Grand Cayman Island
5) Charley (2)	130	941	8/13/2000	Punta Gorda, FL
6) Wilma	130	927	9/22/2145	Cozumel, Mexico
7) Iris	125	948	10/9/0200	Belize
8) Floyd	120	930	8/14/1900	Bahamas
9) Michelle	120	49	11/4/1800	Cuba
10) Dennis	120	941	7/8/1845	Cuba
11) Luis	115	945	9/5/1200	Barbuda; St. Martin
12) Emily (2)	115	955	7/18/0630	Tulum, Mexico
13) Wilma (2)	115	933	9/22/0330	Puerto Morelos, Mexico
14) Isidore '02	110	936	9/22/2100	Yucatan, Mexico
15) Lenny (2)	110	966	11/18/1800	St. Martin
16) Frances	110	948	9/2/2000	Bahamas
17) Ivan	110	952	9/7/2200	Grenada
18) Emily (3)	110	944	7/20/1200	San Fernando, Mexico
19) Katrina (2)	110	920	8/29/1110	Buras, LA
20) Georges	105	962	9/22/1200	Dominican Republic
21) Charley	105	966	8/13/0400	Cuba
22) Ivan (5)	105	946	9/16/0700	Gulf Shores, AL
23) Jeanne (3)	105	950	9/26/0400	Stuart, FL
24) Dennis (2)	105	946	7/10/1930	Navarre Beach, FL
25) Katrina (3)	105	928	8/29/1445	Waveland, MS
26) Wilma (3)	105	950	9/24/1030	Cape Romano, FL
27) Opal	100	942	10/4/1200	Pensacola, FL
28) Bret	100	951	8/23/0000	Padre Island, TX
29) Fabian	100	952	9/5/2000	Bermuda
30) Fran	100	954	9/6/0000	Cape Fear, NC
31) Roxanne	100	958	10/11/0200	Tolum, Mexico
32) Georges (2)	100	966	9/21/0400	Antigua
33) Georges (3)	100	968	9/21/2200	Puerto Rico
34) Jeanne (2)	100	956	9/25/1400	Bahamas
35) Rita	100	937	9/24/0740	Johnson's Bayou, LA; Sabine Pass, TX
36) Bonnie	95	964	8/27/0400	Wilmington, NC
37) Floyd (2)	90	956	8/16/0600	Cape Fear, NC
38) Isabel	90	957	9/18/1700	Drum Inlet, NC
39) Georges (4)	90	964	9/28/1100	Biloxi, MS
40) Lili '02	90	971	10/01/1400	Cuba
41) Bertha	90	974	7/12/2000	Wilmington, NC
42) Georges (5)	90	981	9/25/1500	Key West, FL
43) Frances (2)	90	960	9/5/0500	South Hutchinson Island, FL
44) Beta	90	970	10/30/1200	Nicaragua
45) Lili '96	85	975	10/18/0900	Cuba
46) Mitch	85	987	10/29/1200	Honduras
47) Michelle (2)	80	973	11/15/1200	Bahamas
48) Keith (2)	80	980	10/5/1800	Tampico, Mexico
49) Isidore '02 (2)	75	964	9/20/2100	Cuba
50) Emily	75	989	7/14/0700	Grenada
51) Marilyn	70	984	9/14/2100	St. Thomas, Virgin Islands
52) Hortense	70	989	9/10/0600	Puerto Rico
53) Jeanne	70	985	9/16/1100	Dominican Republic
54) Charley (3)	70	992	8/14/1400	Cape Romain, SC
55) Katrina	70	984	8/25/2330	North Miami Beach, FL
56) Keith	65	988	10/2/2300	Belize
57) Georges (6)	65	993	9/23/2100	Cuba
58) Alex	65	981	8/3/1800	Cape Hatteras, NC

ments that describe Atlantic major hurricanes. The 1995–2005 period was chosen for its large sample and the availability of the IR satellite archive (Zehr 2000; Mueller et al. 2006). Several interesting points and noteworthy findings are documented by this study. 1) The Atlantic major hurricane activity of the 1995–2005 period distinctly exceeds the long-term average, however the locations and intraseasonal distributions are quite close to the long-term averages. 2) The degrees to which maximum intensity measurements deviate from a pressure–wind relationship are illustrated. 3) The exceptional intensification rates of Hurricane Wilma (2005) are shown with respect to the more typical major hurricane intensification rates. 4) In addition to the satellite intensity estimates using the digital Dvorak technique, the associated component temperatures and cold IR cloud area measurements are documented. 5) Hurricane size as given by the average radius of gale force wind at maximum intensity has an extremely large range from 92.5 to 427.4 km.

This work also illustrates the need for more thorough investigations with expanded datasets on several topics. Specific recommendations are as follows.

1) Deviations of Vmax and MSLP from pressure–wind relationships should be explained according to the hurricane's structure and environment. To do this, the influence of additional measurements such as environmental pressure, size, translation speed, and latitude need to be quantified (Knaff and Zehr 2007). More satellite-based techniques that independently assign MSLP and Vmax (e.g., Demuth et al. 2004, 2006) should be developed for use with both operational and best-track data.
2) IR image–derived quantities have been incorporated into statistical intensity forecasts (DeMaria et al. 2005) and rapid intensification forecasts (Kaplan and DeMaria 2003). Refinements to these approaches should be explored as well as additional satellite-based nowcast and short-term intensity forecast techniques. The valuable information content of the microwave image data (Hawkins et al. 2001) should be combined with the higher spatial and temporal resolution available from the geostationary images.
3) Additional work is needed to perform a thorough validation of the objective Dvorak intensities, including characteristics such as timing of maximum intensity, the timing of rapid intensification, and biases as a function of intensity.
4) Improved use of IR satellite image data for wind radii assignments, including the radius of maximum wind, should be explored. Recent research studies (Mueller et al. 2006; Kossin et al. 2007) have demonstrated that the IR data are potentially useful for operational analyses of tropical cyclone structure.

Acknowledgments. This work is supported by NOAA Grants NA90RAH00077 and NA17RJ1228. We thank the anonymous reviewers for their comments on improving the manuscript. The views, opinions, and findings in this article are those of the authors and should not be construed as an official NOAA and or U.S. government position, policy, or decision.

REFERENCES

DeMaria, M., M. Mainelli, L. K. Shay, J. A. Knaff, and J. Kaplan, 2005: Further improvements to the Statistical Hurricane Intensity Prediction Scheme (SHIPS). *Wea. Forecasting,* **20,** 531–543.

Demuth, J. L., M. DeMaria, J. A. Knaff, and T. H. Vonder Haar, 2004: Evaluation of Advanced Microwave Sounding Unit tropical cyclone intensity and size estimation algorithms. *J. Appl. Meteor.,* **43,** 282–296.

——, ——, and ——, 2006: Improvement of Advanced Microwave Sounding Unit tropical cyclone intensity and size estimation algorithms. *J. Appl. Meteor. Climatol.,* **45,** 1573–1581.

Dvorak, V. F., 1975: Tropical cyclone intensity analysis and forecasting from satellite imagery. *Mon. Wea. Rev.,* **103,** 420–430.

——, 1984: Tropical cyclone intensity analysis using satellite data. NOAA Tech. Rep. NESDIS 11, U.S. Department of Commerce, Washington, DC, 47 pp.

Elsner, J. B., and A. B. Kara, 1999: *Hurricanes of the North Atlantic: Climate and Society*. Oxford University Press, 488 pp.

——, ——, and M. A. Owens, 1999: Fluctuations in North Atlantic hurricane frequency. *J. Climate,* **12,** 427–437.

——, T. Jagger, and X.-F. Niu, 2000a: Changes in the rates of North Atlantic major hurricane activity during the 20th century. *Geophys. Res. Lett.,* **27,** 1743–1746.

——, K. Liu, and B. Kocher, 2000b: Spatial variations in major U.S. hurricane activity: Statistics and a physical mechanism. *J. Climate,* **13,** 2293–2305.

——, X. Niu, and T. H. Jagger, 2004: Detecting shifts in hurricane rates using a Markov chain Monte Carlo approach. *J. Climate,* **17,** 2652–2666.

Emanuel, K., 2005: Increasing destructiveness of tropical cyclones over the past 30 years. *Nature,* **436,** 686–688.

Erickson, C. O., 1972: Evaluation of a technique for the analysis and forecasting of tropical cyclone intensities from satellite pictures. NOAA Tech. Memo. NESS 42, Springfield, VA, 28 pp.

Goldenberg, S. B., and L. J. Shapiro, 1996: Physical mechanisms for the association of El Niño and West African rainfall with Atlantic major hurricane activity. *J. Climate,* **9,** 1169–1187.

——, C. W. Landsea, A. M. Mesta-Nuñez, and W. M. Gray, 2001: The recent increase in Atlantic hurricane activity: Causes and implications. *Science,* **293,** 474–479.

Gray, W. M., 1984: Atlantic seasonal hurricane frequency. Part I: El Niño and 30 mb quasi-biennial oscillation influences. *Mon. Wea. Rev.,* **112,** 1649–1668.

——, P. J. Klotzbach, and W. Thorson, cited 2005: Extended range forecast of Atlantic seasonal hurricane activity and

U.S. landfall strike probability for 2005. [Available online at http://hurricane.atmos.colostate.edu.]

Guard, C. P., and M. A. Lander, 1996: A wind-pressure relationship for midget TCs in the western North Pacific. 1996 Annual Tropical Cyclone Rep., Naval Pacific Meteorology and Oceanography Center/Joint Typhoon Warning Center, 311 pp. [Available online at https://metocph.nmci.navy.mil/jtwc/atcr/1996atcr/pdf/1996.html.]

——, L. E. Carr, F. H. Wells, R. A. Jeffries, N. D. Gural, and D. K. Edson, 1992: Joint Typhoon Warning Center and the challenges of multibasin tropical cyclone forecasting. *Wea. Forecasting,* **7,** 328–352.

Harper, B. A., 2002: Tropical cyclone parameter estimation and the Australian region: Wind-pressure relationships and related issues for engineering planning and design—A discussion paper. SEA Rep. J0106-PR003E, 83 pp. [Available from Systems Engineering Australia Pty. Ltd., 7 Mercury Ct., Bridgeman Downs, QLD 4035, Australia.]

Hawkins, J. D., T. F. Lee, J. Turk, C. Sampson, J. Kent, and K. Richardson, 2001: Real-time Internet distribution of satellite products for tropical cyclone reconnaissance. *Bull. Amer. Meteor. Soc.,* **82,** 567–578.

——, M. Helveston, T. F. Lee, F. J. Turk, K. Richardson, C. Sampson, J. Kent, and R. Wade, 2006: Tropical cyclone multiple eyewall configurations. Preprints, *27th Conf. on Hurricanes and Tropical Meteorology,* Monterey, CA, Amer. Meteor. Soc., 6B.1.

Holland, G. J., 1980: An analytic model of the wind and pressure profiles in hurricanes. *Mon. Wea. Rev.,* **108,** 1212–1218.

Jarvinen, B. R., and C. J. Neumann, 1979: Statistical forecasts of tropical cyclone intensity for the North Atlantic basin. NOAA Tech. Memo. NWS NHC-10, 22 pp.

Kalnay, E., and Coauthors, 1996: The NCEP/NCAR 40-Year Reanalysis Project. *Bull. Amer. Meteor. Soc.,* **77,** 437–471.

Kaplan, J., and M. DeMaria, 2003: Large-scale characteristics of rapidly intensifying tropical cyclones in the North Atlantic basin. *Wea. Forecasting,* **18,** 1093–1108.

Knaff, J. A., and R. M. Zehr, 2007: Reexamination of tropical cyclone wind–pressure relationships. *Wea. Forecasting,* **22,** 71–88.

Kossin, J. P., J. A. Knaff, H. I. Berger, D. C. Herndon, T. A. Cram, C. S. Velden, R. J. Murnane, and J. D. Hawkins, 2007: Estimating hurricane wind structure in the absence of aircraft reconnaissance. *Wea. Forecasting,* **22,** 89–101.

Landsea, C. W., 1993: A climatology of intense (or major) Atlantic hurricanes. *Mon. Wea. Rev.,* **121,** 1703–1713.

——, N. Nicholls, W. M. Gray, and L. A. Avila, 1996: Downward trends in the frequency of intense Atlantic hurricanes during the past five decades. *Geophys. Res. Lett.,* **23,** 1697–1700.

——, R. A. Pielke Jr., A. M. Mestas-Nunez, and J. A. Knaff, 1999: Atlantic basin hurricanes: Indices of climatic changes. *Climatic Change,* **42,** 89–129.

Love, G., and K. Murphy, 1985: The operational analysis of tropical cyclone wind fields in the Australian northern region. Northern Territory Region Research Papers 1984–1985, Bureau of Meteorology, 44–51. [Available from National Meteorological Library, GPO Box 1289, Melbourne, VIC, 3001, Australia.]

Maclay, K. S., 2006: Tropical cyclone inner core energetics and its relation to storm structural changes. Preprints, *27th Conf. on Hurricanes and Tropical Meteorology,* Monterey, CA, Amer. Meteor. Soc., 2B.1. [Available online at http://ams.confex.com/ams/pdfpapers/108304.pdf.]

Mueller, K. J., M. DeMaria, J. Knaff, J. P. Kossin, and T. H. Vonder Haar, 2006: Objective estimation of tropical cyclone wind structure from infrared satellite data. *Wea. Forecasting,* **21,** 990–1005.

Neumann, C. J., B. R. Jarvinen, C. J. McAdie, and G. R. Hammer, 1999: *Tropical Cyclones of the North Atlantic Ocean, 1871–1998.* NOAA Historical Climatology Series 6-2, National Oceanic and Atmospheric Administration, 206 pp. [Available from National Climatic Data Center, Asheville, NC 28801-5001.]

Olander, T. L., and C. S. Velden, 2004: The Advanced Objective Dvorak Technique (AODT)—Continuing the journey. Preprints, *26th Conf. on Hurricanes and Tropical Meteorology,* Miami, FL, Amer. Meteor. Soc., 224–225.

——, and ——, 2007: The advanced Dvorak technique: Continued development of an objective scheme to estimate tropical cyclone intensity using geostationary infrared satellite imagery. *Wea. Forecasting,* **22,** 287–298.

Pasch, R., E. S. Blake, H. D. Cobb III, and D. P. Roberts, 2006: Tropical cyclone report: Hurricane Wilma, 15–25 October 2005. 27 pp. [Available online at http://www.nhc.noaa.gov/2005atlan.shtml.]

Saunders, M. A., R. E. Chandler, C. J. Merchant, and F. P. Roberts, 2000: Atlantic hurricanes and NW Pacific typhoons: ENSO spatial impacts on occurrence and landfall. *Geophys. Res. Lett.,* **27,** 1147–1150.

Simpson, R. H., 1974: The hurricane disaster potential scale. *Weatherwise,* **27,** 169–186.

Velden, C. S., T. Olander, and R. Zehr, 1998: Development of an objective scheme to estimate tropical cyclone intensity from digital geostationary satellite infrared imagery. *Wea. Forecasting,* **13,** 172–186.

——, and Coauthors, 2006: The Dvorak tropical cyclone intensity estimation technique: A satellite-based method that has endured for over 30 years. *Bull. Amer. Meteor. Soc.,* **87,** 1195–1210.

Weatherford, C. L., and W. M. Gray, 1988: Typhoon structure as revealed by aircraft reconnaissance. Part II: Structural variability. *Mon. Wea. Rev.,* **116,** 1044–1056.

Webster, P. J., G. J. Holland, J. A. Curry, and H.-R. Chang, 2005: Changes in tropical cyclone number, duration, and intensity in a warming environment. *Science,* **309,** 1844–1846.

Willoughby, H. E., J. A. Clos, and M. E. Shoreibah, 1982: Concentric eye walls, secondary wind maxima, and the evolution of the hurricane vortex. *J. Atmos. Sci.,* **39,** 395–411.

——, J. M. Masters, and C. W. Landsea, 1989: A record minimum sea level pressure observed in Hurricane Gilbert. *Mon. Wea. Rev.,* **117,** 2824–2828.

Wilson, R. M., 1999: Statistical aspects of major (intense) hurricanes in the Atlantic basin during the past 49 hurricane seasons (1950–1998): Implications for the current season. *Geophys. Res. Lett.,* **26,** 2957–2960.

Zehr, R. M., 2000: Tropical cyclone research using large infrared image data sets. Preprints, *24th Conf. on Hurricanes and Tropical Meteorology,* Fort Lauderdale, FL, Amer. Meteor. Soc., 486–487.